Utilizing Micro Simulation to Evaluate the Safety and Efficiency of the Expressway System

SAFETY RESEARCH USING SIMULATION

UNIVERSITY TRANSPORTATION CENTER

Jaeyoung Lee, Ph.D., PI

Research Assistant Professor

Mohamed Abdel-Aty, Ph.D., Co-PI
Professor & Chair

Ling Wang, Ph.D.

Utilizing Micro Simulation to Evaluate the Safety and Efficiency of the Expressway System

Jaeyoung Lee, Ph.D., PI

Safety Program Director & Research Assistant Professor

Center for Advanced Transportation Systems Simulation

Department of Civil, Environmental and Construction Engineering

University of Central Florida

Mohamed Abdel-Aty, Ph.D., Co-PI

Pegasus Professor & Chair

Department of Civil, Environmental and Construction Engineering

University of Central Florida

Ling Wang, Ph.D.

Post-doctoral Associate

Department of Civil, Environmental and Construction Engineering

University of Central Florida

A Report on Research Sponsored by SAFER-SIM

August 2016

Table of Contents

List of Figures

List of Tables

Abstract

Expressways play a vital role in serving mega-cities, and the safety of expressways is extremely important. In order to explore the crash mechanisms of expressways, previous studies have mainly utilized average daily traffic (ADT) as a major contributing factor. In recent years, several researchers also adopted average hourly traffic (AHT) and microscopic traffic at five-minute intervals in expressway safety analyses. Nevertheless, there have been no studies, which have compared the performance of all three factors: ADT, AHT, and microscopic traffic.

This study collected data from three expressways in Central Florida, including traffic data at one-minute intervals, detailed crash information, and geometric characteristics. A Bayesian Poisson-lognormal model was estimated for total crash frequency using ADT, a Bayesian multilevel Poisson-lognormal model was built for hourly crash frequency prediction using AHT, and a Bayesian multilevel logistic regression model was developed for real-time safety analysis using microscopic traffic indicators at five-minute intervals. The modeling results showed that the crash-contributing factors found by different models were comparable but not the same. Four variables, i.e., the logarithm of volume, segment length, number of lanes, and existence of weaving segments, were found to be positively significant in the three models, and four other variables were only significant in one or two models. The ADT-based, AHT-based, and five-minute-based models were used to predict safety conditions at different levels: total, hourly, and five-minute intervals. The results indicated that the AHT-based crash-estimation model performed the best in predicting total and hourly crash frequency, and that the real-time crash prediction model was the best in identifying crash events for dangerous segments at five-minute intervals. The AHT was recommended for future long-term traffic safety analysis, and traffic at five-minute intervals was suggested for the implementation of active traffic management (ATM).

Since the existence of weaving segments was found to be significantly related to crash potential in all three crash analyses models, crash-contributing factors of weaving segments were further studied using real-time safety analysis, which implements traffic at five-minute intervals to predict crash potential. This study presents a logistic regression model for crashes at expressway weaving segments using crash data, geometric data, traffic data at one-minute intervals, and weather data. The results show that the speed difference between the beginning and the end of the weaving segment and the logarithm of volume have significant impacts on the crash risk of the following five to ten minutes for weaving segments. The configuration is also an important factor. The weaving segment, in which there is no need for on- or off-ramp traffic to change lanes, presents a high crash risk because there are more traffic interactions and greater speed differences between weaving and non-weaving traffic. Meanwhile, weaving influence length, which measures the distance at which weaving turbulence no longer has impact, is found to be positively related to the crash risk at the 5% confidence interval. In addition to traffic and geometric factors, the wet pavement surface condition significantly increases the crash risk since vehicles are more likely to be out of control and need longer braking distances on wet pavement. Once the crash mechanism of weaving segments was found, the safety condition of weaving segments could be estimated using traffic, geometry, and weather factors at five-minute intervals.

This study focused on the safety of a congested weaving segment, which has a high crash potential. Various ATM strategies were tested in microscopic simulation (VISSIM) through the Component Object Model (COM) interface. The strategies included ramp metering (RM) strategies, variable speed limit (VSL) strategies, and an integrated RM and VSL (RM-VSL) strategy. Overall, the results showed that the ATM strategies were able to improve the safety of the studied weaving segment. The modified ALINEA RM algorithms, which took both lane occupancy and safety into consideration, outperformed the traditional ALINEA algorithm from a safety point of view but at the expense of average travel time. The 45 mph VSLs, which were located at the upstream of the studied weaving segment, significantly enhanced the safety without notably increasing the average travel time. In order to reduce the average travel time of the modified ALINEA RM and maintain its impact on safety, the modified ALINEA RM was adjusted to control queue length and was integrated with the 45 mph VSL strategy. The simulation results have proved that the consolidated RM-VSL approach yields slightly lower total crash risks, but provides much lower average travel times than the modified ALINEA.

Overall, the existence of a weaving segment would significantly increase crash potential, and the traffic at five-minute intervals was suitable for the implementation of ATM. Based on these two findings, a congested weaving segment was chosen to test the impact of ATM on safety in real time through microscopic simulation. The result showed that ATM was able to significantly improve the safety of the studied weaving segment.

1 Introduction

Expressways play a vital role in serving mega-cities. They increase the travel speed and reduce the travel time for daily traffic, especially for medium to long trips. If a crash occurs on an expressway, it might bring about two serious consequences: 1) a more severe crash because crash severity is highly related to speed limits, and the speed limits on expressways are usually high; and 2) more congestion because expressways are access controlled, and it might be hard for vehicles to easily change their route. Hence, reducing the crash potential of an expressway is a worthwhile goal.

Previous safety analyses of expressways were mainly based on average daily traffic (ADT). In recent years, with the development of data collection technologies and data processing capabilities, more detailed traffic data, for example, average hourly traffic (AHT) and microscopic traffic data at five-minute intervals, has become available. However, there have not been enough studies, which compare these types of safety analyses, which are based on different traffic data.

Different expressway segment types have different crash potentials. Meanwhile, crash characteristics on different segment types is not the same. When practitioners set out to improve the safety of an expressway, it is hard to take the whole expressway as a subject because not all segments experience high crash frequencies, and because budgets are always limited. Hence, there is a need to first find the most dangerous segment type. Then, the crash-contributing factors of the most dangerous segment type should be closely explored.

Once the crash-contributing factors have been found, several countermeasures can be applied to expressways to improve traffic safety. One of the possible countermeasures is active traffic management (ATM), which is able to dynamically manage roadway facilities to change the traffic conditions and further improve the safety of an expressway segment. In this project, to test the impact of ATM on the safety of expressway segments, microscopic simulation was used. The simulation is a cost-effective way to evaluate traffic safety in simulated scenarios, which allows researchers and practitioners to test proposed improvement strategies. VISSIM is a widely used microscopic road traffic simulation that is able to simulate the behavior of individual vehicles. Hence, the simulated traffic network can be analyzed in detail. Additionally, in VISSIM, an interface (the Component Object Model interface) is offered. Through the interface, users are able to manipulate the attributes of internal objectives dynamically, such as speed limit and ramp signal timing.

The main objective of this study was to improve the safety of an expressway system based on safety analysis and microscopic simulation. To achieve the proposed objective, several tasks were carried out.

- Task 1: Evaluating the stability of the three types of safety analyses in identifying the important contributing factors and their ability to use the identified variables to predict safety conditions;

- Task 2: Identifying the most dangerous expressway segment type based on safety analyses using ADT, AHT, and microscopic data;
- Task 3: Exploring the crash mechanism of the most dangerous expressway segment type using real-time safety analysis;
- Task 4: Building a well-calibrated and validated VISSIM network for an expressway segment with high crash potential; and
- Task 5: Testing the impact of ATM on the safety of the expressway segment identified by Task 4.

Following this chapter, this report begins with a literature review on existing crash analysis and ATM strategies in Chapter 2. Chapter 3 describes the data that were collected, including crash, traffic, road geometric characteristics, and weather data. Chapter 4 focuses on safety analysis of an expressway system based on traffic data aggregated at different levels: ADT, AHT, and microscopic traffic. Chapter 5 conducted a real-time safety analysis for weaving segments, which were identified as the most dangerous segment type by Chapter 4. Chapter 6 and 7 build a microscopic simulation, VISSIM network for a congested weaving segment and apply ATM to reduce the crash risk on the segment. Conclusions are summarized in Chapter 8.

2 Literature Review

This chapter presents the literature review in two parts: crash analyses and ATM strategies. In the first part, crash analyses based on different traffic data are summarized to illustrate which crash analysis might be suitable in safety analysis of expressway segments. In the second part, two main ATM strategies, i.e., variable speed limit (VSL) and ramp metering (RM), have been reviewed with a focus of the impact of ATM on traffic safety.

2.1 Crash Analyses

The cause-effect relationship between crashes and traffic conditions has been widely explored based on ADT or annual average daily traffic (AADT). However, some researchers have stated that the cause-effect relationship actually should be between a crash and the traffic conditions prevailing near the time of crash occurrence, or else there might be a biased result due to the implementation of AADT (Mensah & Hauer, 1998). Hence, AHT and microscopic traffic data at five-minute intervals, which are closer to the time of crash occurrence than AADT, have been used in crash analysis.

Average-hourly-traffic-based traffic safety studies were first conducted by Gwynn (1967). The author found a U-shape relationship between crash rate and hourly volume: high crash rates occurred at low and high hourly volumes and low crash rates at median hourly volumes. Later, Ceder (1982) used power functions to examine the relationship between hourly traffic flows and hourly crash rate because it was noted that ADT failed to explain the relationship between traffic and crashes. In that study, different crash types (single- and multi-vehicle crashes) under different traffic conditions (free- and congested-flow conditions) were studied separately. Then, Persaud and Dzbik (1993) implemented generalized linear models and the empirical Bayesian method to estimate crash frequency using hourly volume and ADT individually. However, in their study, hourly traffic volumes were estimated on the basis of ADT. Martin (2002) explored the relationship between crash rates and hourly volume and investigated the impact of volume on crash severity.

Other hourly traffic parameters were also used to estimate hourly crashes. Lord et al. (2005) applied hourly vehicle density and volume over capacity (v/c) in hourly crash frequency prediction for rural and urban freeways. Their results showed that vehicle density and v/c ratio were positively related to hourly crash frequency. Zhou and Sisiopiku (1997) used parabolic equations to explain the relationship between v/c and crash rates for different crash types, for example, multi-vehicle crashes and rear-end crashes. Chang et al. (2000) explored the relationship between crash rate and hourly v/c. In their research, three types of freeway segments were studied: basic freeway sections, tunnel sections, and toll gate sections. U-shape relationships between crash rate and hourly v/c were also found for these three sections.

Compared to the hourly crash study, there are many more real-time safety studies. It has become one of the most heavily studied traffic safety topics, since it was first examined in 1995 (Madanat and Liu, 1995). The subjects of real-time safety studies covered freeway mainlines (Lee et al., 2002; Abdel-Aty et al., 2004; Pande et al., 2005), ramp vicinities (Hossain & Muromachi, 2013a, b), ramps (Lee & Abdel-Aty, 2006; Wang et al., 2015b), and weaving

segments (Wang et al., 2015a). With more and more efforts in real-time safety analysis, researchers explored different crash types in real time, including single-vehicle crashes and multi-vehicle crashes (Yu & Abdel-Aty, 2013); explored crash-contributing factors under different conditions, i.e., high- and low-speed conditions (Abdel-Aty et al., 2005). Crash contributing factors discovered by former studies mainly included traffic (Hossain & Muromachi, 2013b), roadway geometric characteristics (Yu & Abdel-Aty, 2013), and weather (Abdel-Aty & Pemmanaboina, 2006).

Almost all previous real-time safety analyses implemented case-control design to randomly select some non-crash events to represent the non-crash population. The main reason for the wide use of case-control design was that the number of non-crash events is always much greater than that of crash events. Some of these studies adopted the matched-case-control design to exclude the impact of geometry and time of day on crash occurrence (Pande et al., 2005; Abdel-Aty & Pemmanaboina, 2006). The main statistical method of real-time crash estimation is the logistic regression model (Abdel-Aty & Pemmanaboina, 2006; Hourdos et al., 2006; Zheng et al., 2010). Additionally, several data mining methods have been used: Bayesian belief net (Hossain & Muromachi, 2013a, b), support vector machine (Qu et al., 2012), and multilayer perceptron neural network (Pande et al., 2011). The data mining method may provide better model performance, but on the other hand, it might not be able to provide the quantitative impact of a significant variable on crash occurrence.

To summarize, AHT-based and real-time safety analyses might outperform ADT-based safety studies; there have been several hourly and real-time safety studies, but little to no research has compared ADT-based, AHT-based, and five-minute-based crash analyses. Case-control design has been widely implemented in real-time safety analyses.

2.2 ATM Strategies

Active traffic management is mainly designed to enhance traffic operation, for example, increasing roadway capacity and improving travel time reliability. The ATM strategies include VSL, hard shoulder running, RM, etc. Among these strategies, RM and VSL have been widely used and have been proven to have a significantly positive impact on traffic safety.

The basic concept of the RM algorithm is adjusting on-ramp entering volume based on the mainline's traffic operational conditions (Papageorgiou & Kotsialos, 2000). Ramp metering has facilitated freeway operations in the following aspects: decreasing travel time and increasing travel time reliability (Bhouri & Kauppila, 2011), alleviating traffic congestion (Haj-Salem & Papageorgiou, 1995), and increasing capacity (Cassidy & Rudjanakanoknad, 2005), etc. Additionally, RM has significant impact on traffic safety. The Minnesota Department of Transportation (Cambridge Systematics Inc., 2001) found a 26% increase in crash frequency after the RMs were off. Michalopoulos et al. (2005) inferred that RM could potentially decrease freeway crash rates since it significantly reduced the total number of mainline stops. Several studies have explored the safety impact of RM from a microscopic aspect as well. Lee et al. (2006) quantified the effects of local traffic-responsive ALINEA RMs on freeway real-time safety and concluded that RMs reduced crash potential by 5–37%. Later, Abdel-Aty et al. (2007) adopted RMs on a congested freeway and found that RMs significantly decreased crash risk.

Abdel-Aty and Gayah (2008) also successfully adopted an uncoordinated ALINEA and a coordinated zone ramp metering algorithm to mitigate real-time crash risk.

Variable speed limits adjust speed limits based on different traffic and weather conditions. They can possibly improve traffic safety and mitigate traffic congestion by adjusting vehicles' speed and decreasing speed variation among vehicles (Li et al., 2014). Variable speed limits have the potential benefit of improving traffic operations. Previous research has confirmed that the throughputs and capacity of networks have been increased because of VSLs (Kwon et al., 2007). Another advantage of VSL is reducing speed variances. Several experiments have studied the speed variance after implementing VSL through driving simulators (Lee & Abdel-Aty, 2008) and simulations (Kang & Chang, 2011). These experiments' results were the same as what has been observed in the field (Rämä, 1999): drivers drove at more homogeneous speeds with the VSL than with the static speed limits. Reducing speed variance indicates a lower crash likelihood (Hossain & Muromachi, 2010), so VSL might improve safety. Saha and Young (2014) collected six winter seasons' worth of data and concluded that VSL significantly reduced winter crashes by 0.67 crashes per week per 100 miles over that period. Yet collecting enough crash data is not practical in all cases since it takes a long time because the occurrence of a crash is infrequent. Therefore, there have been several studies, which have conducted safety studies of VSL in simulation (Lee et al., 2004; Abdel-Aty et al., 2006; Yu & Abdel-Aty, 2014). These studies have utilized one or several precursors, such as speed variation, to calculate crash risk. Their results have demonstrated that VSL is an effective strategy to mitigate crash risk.

However, the success of VSL is dependent on the level of compliance (Yu & Abdel-Aty, 2014). If drivers do not follow the new speed limit, the VSL would fail to improve traffic safety. The coordination of RM and VSL might be an approach to avoid the failure of ATM. Even if the VSL strategy does not work, the RM is still able to improve traffic safety. Meanwhile, RM is able to regulate on-ramp traffic, and VSL can change mainline traffic conditions. Hence, the coordination of RM and VSL is able to change the traffic conditions of the on-ramp and mainline simultaneously, and might further improve the safety of a weaving segment network. Compared to the RM and the VSL, the integrated RM and VSL strategy might result in a network that has a higher outflow or a significantly lower total travel time or both (Hegyi et al., 2005). Previous studies have found that the integrated strategy is able to significantly prevent congestion, improve stability, or reduce delays (Lu et al., 2011). Furthermore, the safety benefit of the integrated strategy is noteworthy. Abdel-Aty and Dhindsa (2007) implemented VSLs and RMs on congested freeway segments. They concluded that the integrated strategy outperforms VSLs or RMs alone in terms of safety, speed, and travel time. Later, Abdel-Aty et al. (2009) also applied VSL and RM to reduce crash risk on freeway segments under congested and uncongested conditions. It was found that the integrated strategy provides lower crash risk than VSL only at the 80% volume load.

Overall, the safety benefits of RM and VSL have been confirmed from theoretical and practical aspects. Meanwhile, the integrated RM and VSL strategy might outperform both RM and VSL by improving traffic operation and crash risk. Nevertheless, previous studies, which adopted the traditional ALINEA algorithm to reduce crash risk in simulation, have not incorporated safety in

the algorithm when deciding the RM rate. Meanwhile, the previous studies did not focus on applying ATM to a special expressway facility that has a high crash potential.

3 Big Data Collection and Processing

The Central Florida Expressway Authority (CFX) operates and maintains 109 miles of expressway networks in Central Florida. Currently, there are five toll roads under or partly under the management of CFX. The expressway networks connect Orlando and neighboring areas, serving both residents and visitors. This project studies the three most important expressways (SR 408, SR 417, and SR 528). The locations of the study's three expressways are shown in Figure 3.1.

Source: Central Florida Expressway Authority, Central Florida Expressway Map (CFX, 2016)

Figure 3.1 – Studied expressways.

In order to find the crash-contributing factors and then to find potential countermeasures to improve the safety of expressway segments, four data sources were collected and processed. They were crash, traffic, road geometric characteristics, and weather data.

3.1 Crash Data

In Florida, crashes are recorded in two formats of crash reports, namely the short form and the long form. Long-form crash reports are designed to keep records of more severe crashes, especially those involving injuries or fatalities. Short-form crash reports are mostly used for property-damage-only crashes. The Signal Four Analytics (S4A) data served as the crash data source of this project. One issue with the S4A database is that for the crashes that occurred in early years (e.g., early 2000s), the short-form crash reports were not complete. After June 2012, S4A has the complete crash data from both types of reports for all of Florida. This research is based on the data after July 2013; thus, there is no issue with the crash data.

The crashes contained in S4A are geocoded data with longitude and latitude, but crash direction and roadway milepost are not available. To locate these crashes and assign direction and milepost information, a geographic information system (GIS) network specifically for the expressways was created using ArcGIS. The original GIS data was downloaded from the Florida Department of Transportation (FDOT) website. The research team made adjustments to keep only the expressways, as shown in Figure 3.2.

Then, to locate the crashes on the expressways, all of the crashes occurring within Orange County during the study period were first selected. Figure 3.3 gives an example of the crashes in Orange County in 2013. Then an initial selection of crashes on the expressways was made.

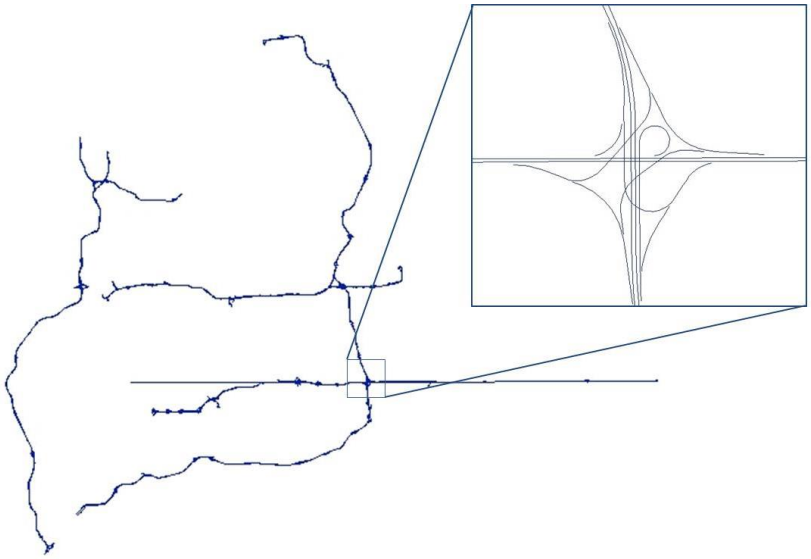

Figure 3.2 – CFX expressway network in GIS.

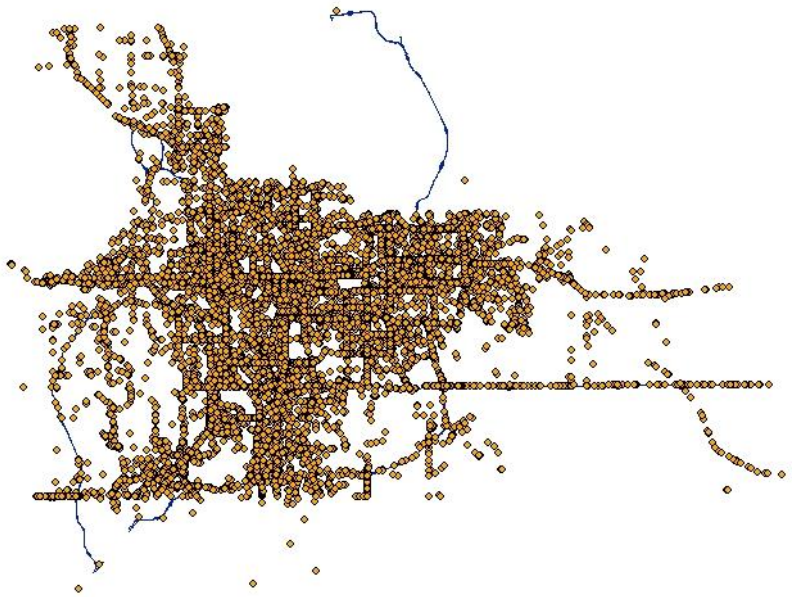

Figure 3.3 – Total crashes in Orange County in 2013.

In the crash report, there is one column indicating the crash street based on which expressways a crash was collected. However, the naming of the expressways is not consistent. As a solution, several key words that could be used for the same expressway were extracted using the structured query language (SQL) technique as shown in Table 3.1. The "%" means any string of zero or more characters, and "_" means any single character within the string in SQL.

Table 3.1 – Key words used for expressway crash selection.

Expressway	Key Words
SR 408	"%408%", "%E-W%", "%E/W%", "%EAST_WEST%", "EW %", "%EASTWEST%"
SR 417	"%417%", "%CENTRAL_FL%", "GREENEWAY"
SR 528	"%528%", "%BEELINE%", "BEACHLINE"

Using these criteria, the initial selection was made as displayed in Figure 3.4. As can be seen in Figure 3.4, the majority of the crashes after the initial selection are located on the CFX expressway systems. A few of the crashes that are not related to the expressways were also included because they share the same key words that are used to filter the expressway crashes. In addition, some crashes on the expressways occurred on the segments that are not operated by CFX. These crashes would also not be included in further analysis.

Therefore, a final selection of the crashes that happened on the studied expressways was conducted by deleting the unrelated crash points in ArcGIS. The results of the final selection are illustrated in Figure 3.5. In this figure, the crashes not related to expressways and those crashes not occurring on segments operated by CFX have been excluded. In the final crash data, crashes on the mainline, ramps, and toll plaza cash lanes on the segments managed by CFX are selected. Figure 3.6 shows the detail about how these crashes are assigned. Both crash direction and mileposts are assigned to the crashes using ArcGIS.

Figure 3.4 – Initial selection of expressway crashes

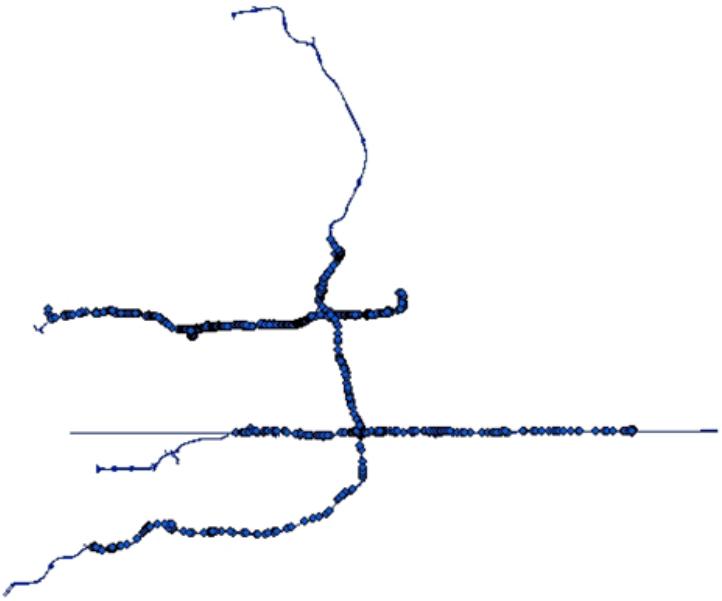

Figure 3.5 – Final selection of expressway crashes.

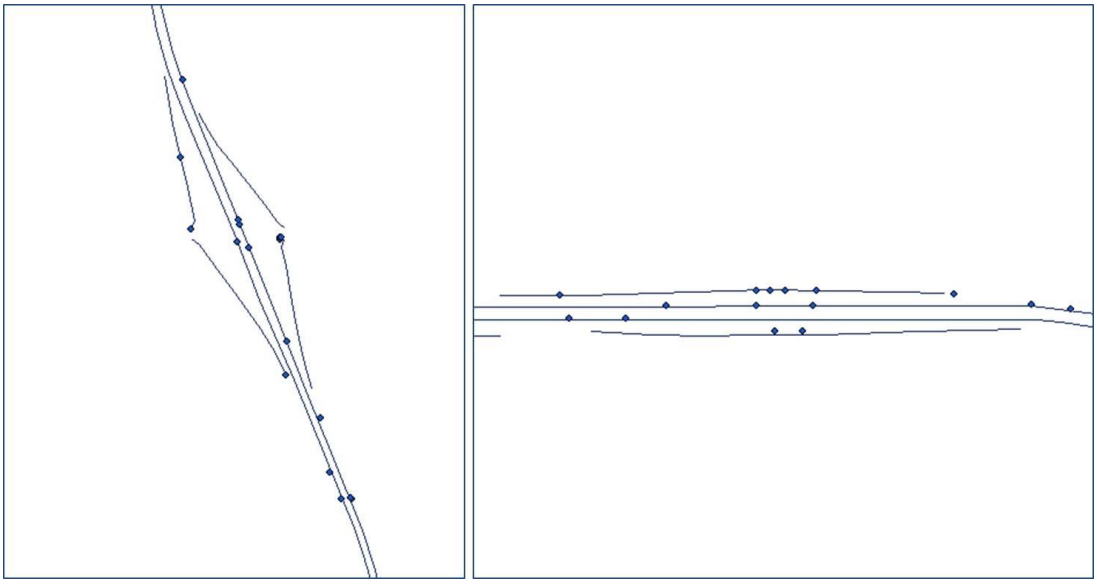

Figure 3.6 – Crash match on mainline, ramp and toll plaza lanes.

Finally, the number of crashes on each expressway is illustrated in Table 3.2. SR 408 has the most crashes, and SR 417 has slightly more crashes than SR 528. One of the most important reasons is that SR 408 is the spine of the system and carries the most traffic. Meanwhile, SR 408 travels through the downtown area of Orlando and needs to provide dense on- and off-ramps to

facilitate downtown traffic. Hence, the spacing between ramps sometimes is limited, and too-short spacing increases crash potential (Ray et al., 2011).

Table 3.2 – Crash number of expressways.

Route	Length (mi)	Year 2013	2014	2015	Average	Crash/mi
SR 408	21.4	700	761	945	758	35.4
SR 417	31.5	355	476	567	442	14.0
SR 528	22.4	313	379	419	347	15.5

3.2 Traffic Data

The traffic data were provided by the Microwave Vehicle Detection System (MVDS), which was initially introduced to CFX's expressways in 2012 specifically for traffic monitoring. The whole network operated by CFX was covered by MVDS as displayed in Figure 3-7.

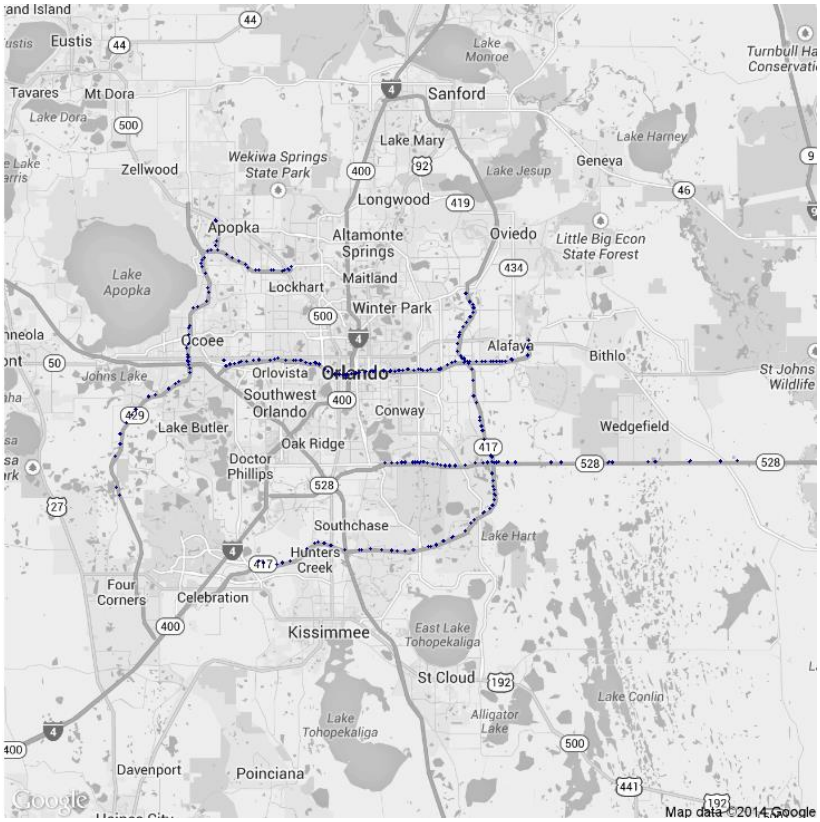

Figure 3.7 – Deployment of MVDS sensors on the expressway network.

For the purpose of this project, MVDS data have been collected since July 2013. MVDS detectors do not identify individual vehicles. They return aggregated traffic flow parameters for each lane of each section, where the MVDS detector is installed, at one-minute intervals. The traffic parameters include traffic volume, time mean speed, lane occupancy, and traffic volume by vehicle length. Four types of vehicles were defined by their lengths:

- Type 1: vehicles 0 to 10 feet in length
- Type 2: vehicles 10 to 24 feet in length
- Type 3: vehicles 24 to 54 feet in length
- Type 4: vehicles over 54 feet in length

Additional information on traffic data from MVDS detectors includes the timestamp when the sensor is polled. It was mentioned earlier that the sensors are polled every one minute. Also, unique sensor identifiers and lane identifiers are contained within the data. The sensor identifier consists of the roadway (i.e., SR 408, SR 417, or SR 528), milepost, and direction. The lanes are counted from the roadway medium to the outside lane. The lanes fall into four categories: Mainline, Ramp, Mainline TP Express, and Mainline TP Cash. Mainline TP Expressway indicates express lanes at mainline toll plazas; vehicles equipped with tags do not need to slow down on these lanes when they pass the toll plazas. Mainline TP Cash means toll booths at mainline toll plazas; vehicles need to stop and pay tolls. On the expressways, these two types of lanes are physically separated. Table 3.3 gives an example of the lane types and numbers at each MVDS detection on eastbound SR 408. The detector information for other roadways can be found in **Appendix A**.

Table 3.3 – SR 408 eastbound MVDS system and lane configuration.

Eastbound		Number of lanes			Eastbound		Number of lanes		
ID	Milepost	Mainline (w/ TP Express)	TP Cash	Ramp	ID	Milepost	Mainline (w/ TP Express)	TP Cash	Ramp
1	1.2			2	30	11.5	5		1
2	1.4	2			31	12.1	5		
3	1.7	2		2	32	12.5	5		1
4	2.2	3		1	33	12.9	5		2
5	2.4	3		1	34	13.3	5		2
6	2.7	3	2		35	13.7	3	3	
7	3.2	2	1		36	14.2	3	2	
8	3.6	2		1	37	14.5	4		
9	4.3	3		1	38	14.7	4		2
10	4.6	4			39	15	5		
11	4.9	3		1	40	15.7	4		2
12	5.3	3		1	41	15.8	4		1
13	6	3	2	1	42	16.1	4		1
14	6.4	3	1		43	16.5	5		
15	6.8	3			44	17.3	3		3
16	7	3		1	45	17.7	2		1
17	7.4	3			46	18	2		1
18	7.6	3		1	47	18.4	2		1
19	8	3		1	48	18.8	2		1
20	8.4	3		1	49	19	2	2	
21	8.9	3		1	50	19.4	2	1	
22	9.2	3		1	51	19.5	2		1
23	9.4	4		1	52	20.1	2		1
24	9.6	3		1	53	20.3	2		
25	9.7			1	54	20.8	2		1
26	10.3	3		1	55	21.8	2		
27	10.6	4		1	56	22.3	2		2
28	10.8	5		1	57	22.7	2		
29	11.2	5		1					

3.3 Road Geometric Characteristics Data

Roadway geometry has a significant impact on traffic operation and safety. The FDOT maintains the Road Characteristics Inventory (RCI) database, which has roadway geometry and other relevant information. The RCI database has hundreds of road characteristic variables. Only the most relevant geometric variables were chosen for the data preparation. In sum, 15 variables were selected: number of lanes, auxiliary lane type, shoulder type, shoulder width, median width, median type, inside shoulder type, inside shoulder width, horizontal degree of curvature, pavement condition, maximum speed limit, D factor, K factor, truck percentage, and section ADT. Table 3.4 gives an example of the RCI data.

Table 3.4 – RCI data structure.

Roadway Characteristics Inventory																
		Characteristics														
RDWYID	BegPt	NOLANES	AUXLNTYP	SHLDTYPE	SLDWIDTH	MEDWIDTH	RDMEDIAN	ISLDTYPE	ISLDWDTH	HRZDGCRV	PAVECOND	MAXSPEED	AVGDFACT	AVGKFACT	AVGTFACT	SECTADT
75008170	1.417	2		2	10.0	40	31	2	4.0	0	3.50	55	52.70	8.50	2.90	41000
75008170	1.581	2		2	10.0	40	31	2	4.0	0	5.00	65	52.70	8.50	2.90	41000
75008170	2.206	2		2	10.0	40	31	2	4.0	0	5.00	65	52.70	8.50	2.90	52500
75008170	2.455	2		2	10.0	40	13	2	4.0	0	5.00	65	52.70	8.50	2.90	52500
75008170	2.664	2		2	10.0	40	31	2	4.0	0	5.00	65	52.70	8.50	2.90	52500
75008170	2.903	2		2	10.0	40	13	2	4.0	0	5.00	65	52.70	8.50	2.90	52500
75008170	3.078	2		2	10.0	40	31	2	4.0	0	5.00	65	52.70	8.50	2.90	52500
75008170	3.264	2		2	10.0	40	31	2	4.0	0.75	5.00	65	52.70	8.50	2.90	52500
75008170	3.543	2		2	10.0	40	08	2	4.0	0.75	5.00	65	52.70	8.50	2.90	52500
75008170	3.717	2		2	10.0	40	08	2	4.0	0	5.00	65	52.70	8.50	2.90	52500
75008170	3.879	2		2	10.0	40	23	2	4.0	1	5.00	65	52.70	8.50	2.90	52500
75008170	3.980	3		2	10.0	40	23	2	4.0	1	3.50	65	52.70	8.50	2.90	52500
75008170	4.242	3		2	10.0	40	23	2	4.0	0	3.50	65	52.70	8.50	2.90	52500
75008170	4.789	3		2	10.0	40	23	2	4.0	2.75	3.50	65	52.70	8.50	2.90	52500
75008170	5.027	3		2	10.0	40	13	2	4.0	0	3.50	65	52.70	8.50	2.90	52500
75008000	0.382	3		2	10.0	20	06	2	10.0	1.5	3.80	65	52.70	8.50	9.40	46000
75008000	0.640	3	4	2	10.0	20	06	2	10.0	1.5	3.80	65	52.70	8.50	9.40	46000
75008000	0.725	3	4	2	10.0	20	06	2	10.0	0	3.80	65	52.70	8.50	9.40	46000
75008000	0.866	3		2	10.0	20	06	2	10.0	0	3.80	65	52.70	8.50	9.40	46000

The studied expressways were divided into several segments according to the location of on- and off-ramps. If a segment's geometric characteristic was not consistent, then the characteristic was averaged by using length as a weighting value. For example, if the total length of a segment is 1,000 feet, among which a 400-foot-long segment's median width is 40 feet and a 600-foot-long segment's median width is 20 feet, then the average median width is 28 feet.

3.4 Weather Data

The weather data were collected from airport weather stations whose data are maintained by the National Climate Data Center (NCDC). The weather data were monitored continuously, and if the weather parameters did not change, the data would be recorded every one hour. On the other hand, if weather parameters changed, the weather station would record the new weather state. The dataset included the following variables: sky condition, weather type, wind direction and speed, pressure, humidity, temperature, visibility, hourly precipitation, etc. In this study, only hourly precipitation and weather type were used to provide pavement surface condition: wet and dry. The pavement condition is an important crash-contributing factor. On average, from 2002 to 2012 in the United States, twenty-three percent (23%) of crashes were weather-related, and seventy-four percent (74%) of weather-related crashes happened on wet pavement (FHWA, 2014).

At a timestamp, if the hourly precipitation was higher than zero, or weather type contained TS (thunderstorm), RA (rain), or DZ (drizzle), it meant rainy weather condition. Then, it was assumed that the roadway surface condition was wet in the following one hour of this timestamp (Wang et al., 2015b).

4 Safety Analysis of Expressway System

4.1 Introduction

In order to understand crash causes, a significant number of studies have linked traffic safety with crash-contributing factors such as traffic and geometry. Among these research efforts, the majority have been based on highly aggregated traffic data, i.e., AADT and ADT. However, an expressway with high traffic flow during peak hours would have a different crash potential than an expressway with the same ADT but a traffic flow that is evenly spread out throughout the day (Mensah & Hauer, 1998). Meanwhile, the crash occurrence should be more related to the prevailing conditions prior to the crash than to ADT. Hence, in addition to ADT-based safety studies, this project explored crash more closely through hourly crash studies based on AHT and through real-time crash studies based on microscopic traffic at five-minute intervals.

Hourly crash studies average one or several hours' worth of traffic data over a long time and also aggregate crash frequencies in the corresponding hour(s); for example, the AHT from 8:00 A.M. to 9:00 A.M. in 2015, and the number of corresponding crashes that occurred from 8:00 A.M. to 9:00 A.M. in 2015. Then, the study applies models to find the statistical relationship between hourly crash frequency and hourly traffic flow characteristics along with geometric factors (Lord et al., 2005). If an expressway's hourly traffic does not change much during the day, an hourly crash study would be similar to a crash study based on ADT. Nevertheless, expressways generally have peak and non-peak traffic hours, so an AHT-based crash study might outperform an ADT-based crash study.

Real-time crash analyses use each crash as an event, unlike ADT- and AHT-based studies, which use a segment as a unit for frequencies. In a real-time crash analysis, the condition that occurred just before a crash, such as a traffic situation, is considered to be among the contributing factors that led to the crash and is defined as a crash event. On the other hand, if no crash happens, the condition is defined as non-crash event. By comparing crash to non-crash events, crash precursors that are relatively more "crash prone" than others can be identified (Lee et al., 2002; Abdel-Aty et al., 2005). Real-time safety analyses have been broadly used to predict crash hazards in real time and to test the safety impact of ATM, such as RM and VSL (Lee et al., 2006; Yu & Abdel-Aty, 2014).

All three of the above-mentioned types of traffic safety analyses, especially those based on ADT and microscopic traffic at five-minute intervals, have already been widely studied by previous researchers. However, almost all of the previous studies focused only on one of them. There is a need to compare these three types of safety analyses to identify which one is able to provide better crash estimation. The objectives of this chapter are as follows: (1) to identify the different approaches to analyzing safety at the segment level; (2) to evaluate the stability of the three types of safety analyses in identifying the important contributing factors and their ability to use the identified variables to predict safety conditions; (3) to compare the performance of the different modeling approaches; and (4) to evaluate the safety of the different segment types (i.e., basic, weaving, merge, and diverge).

4.2 Data Preparation

The studied segments were from the three studied expressways in Central Florida: SR 408, 417, and 528. The study period was from July 2013 to December 2015, and April 2014 was excluded because traffic data were not available during that month. This study classified segments into four types according to HCM (2010): merge segments, diverge segments, weaving segments, and basic segments. The layouts of merge, diverge, and weaving segments are illustrated in Figure 4.1. Basic segments are other expressway segments that are not among the three types of segments listed in Figure 4.1.

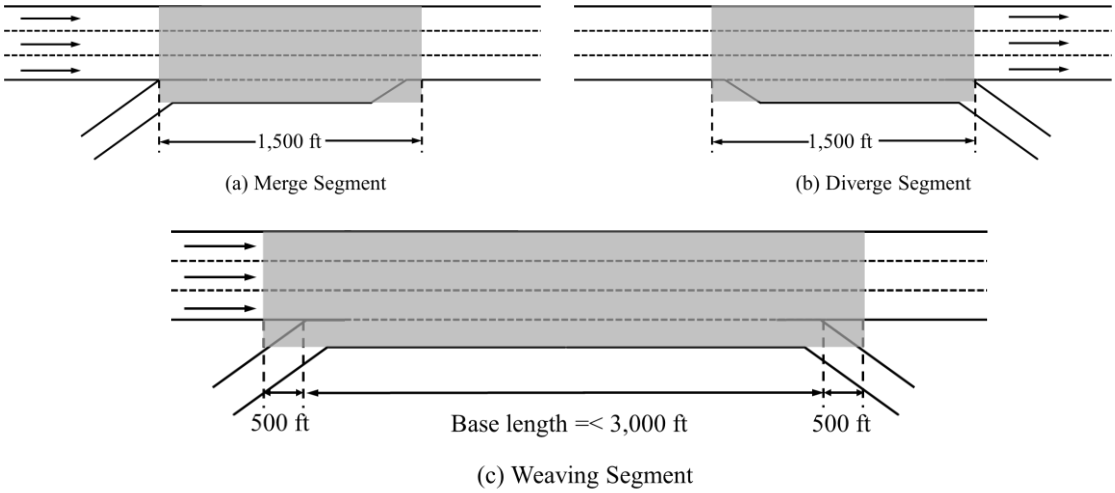

Figure 4.1 – Different segment types.

In total, the three studied expressways have 339 segments. However, not all of these 339 segments were explored. Three sorts of segments were excluded from further analysis, they were toll-plaza-related segments (i.e., the toll plaza and its upstream and downstream segments), segments whose length was less than 500 feet, and segments whose traffic data were not available. The lane configurations of toll-plaza-related segments are very different from other segments; hence, the safety of a toll plaza should not be treated as the same as the other segments and put in the same safety study. For the segments whose length was less than 500 feet, some crashes were on the boundaries of two segments and were randomly assigned to one of the two segments. If a segment is too short, the crash frequency on this segment is usually very low; hence, the random assignment of the crashes on boundaries might have a significant impact on crash frequency results. For example, if the length of a studied segment is 3,000 feet, and five crashes happened in this segment. Adding one crash that happened on the boundary to the studied segment produces six crashes in total. The number of six crashes is just 20% different from the number of five crashes, which is the condition that this boundary crash is assigned to a neighbor segment but not the studied segment. On the other hand, if the length is 400 feet, and one crash happened in this segment. Adding one crash on the boundary to the studied segment produces two crashes in total. The number of two crashes is 100% different

from the number of one crashes, which is the condition that this boundary crash is assigned to a neighbor segment.

Finally, 247 segments were chosen as the study subject, among which 45 were merge segments, 48 were diverge segments, 25 were weaving segments, and 129 were basic segments. The geometric information of the studied segments was mainly obtained from RCI, including number of lanes, speed limit, median width, inside shoulder width, and outside shoulder width. Segment lengths were automatically created by ArcGIS Map. The descriptive analysis of the geometry of studied segments is shown in Table 4.1.

Table 4.1 – Descriptive analysis of the geometric characteristic.

Variables	Mean	Std.	Min.	Max.
Segment length (feet)	3165.65	3396.09	619.08	27652.60
Median width (feet)	46.61	15.30	16	64
Number of lane (lane)	2.66	0.87	0	5
Speed limit (mph)	67.27	4.82	55	70
Inside shoulder width (feet)	7.29	3.56	4	24
Outside shoulder width (feet)	9.64	1.07	2	12

The raw traffic data were obtained from the MVDS, which collected traffic data, including vehicle count, lane occupancy, and speed, for each lane at one-minute intervals. Additionally, the detectors recognized the length of passing vehicles and categorized them under four groups. The vehicle lengths of Groups 3 and 4 were greater than 24 feet; the vehicles in Group 3 and 4 were consider to be trucks, and the total volume of Groups 3 and 4 were used as trucks volume. The traffic data were aggregated into three types: ADT, AHT, and microscopic traffic data at five-minute intervals.

The crash data were from the S4A, which provided detailed crash information, such as crash time, location, severity, and type. The crash characteristics for each segment type are illustrated in Table 4.2. The crash rate of the diverge segment was 1.31, and percentage of rear-end crashes on the diverge segment was 57.7%, which was much higher than that of other segments. An off-ramp vehicle on the diverge segment might decelerate dramatically due to the much lower speed limit on off-ramps than on mainlines. If its following vehicle does not decrease speed in time, a rear-end crash might happen. The crash rate of weaving segments was as high as 0.93 because vehicles merge, diverge, and weave in a limited space (Wang et al., 2015a).

Table 4.2 – Crash characteristic on each segment type.

Crashes	Segment				
	Merge	Diverge	Weaving	Basic	Total
Rear-end crashes	90 (40.0%)	272 (57.7%)	216 (47.3%)	421 (39.2%)	999 (44.8%)
Sideswipe crashes	44 (19.6%)	66 (14.0%)	93 (20.4%)	167 (15.5%)	370 (16.6%)
Off-road crashes	55 (24.4%)	63 (13.4%)	75 (16.4%)	260 (24.2%)	453 (20.3%)
Other crashes	36 (16.0%)	70 (14.9%)	73 (16.0%)	227 (21.1%)	406 (18.2%)
Total	225 (100%)	471 (100%)	457 (100%)	1,075 (100%)	2,228 (100%)
Crash rate (crash frequency/ million vehicle-miles traveled)	0.75	1.31	0.93	0.47	0.65

The geometry, traffic, and crash data were combined. The number of observations in the daily crash analysis dataset was 247, and each segment was an observation. The number of observations in the hourly crash analysis dataset was 5,928, and each segment in one-hour intervals throughout the study period was an observation. The observations in real-time crash analysis were more complicated because there were two types of events: crash and non-crash. Crash events were defined as the conditions 5-10 minutes before the crash occurrence (Hossain & Muromachi, 2013a; Yu & Abdel-Aty, 2013). Hence, if a dangerous traffic condition was predicted, there were five minutes to apply countermeasures to prevent the occurrence of a crash. The non-crash events were based on five-minute intervals. The non-crash events did not result in a crash nor were they impacted by a crash. In order to ensure the purity of non-crash events, all observations within five hours of crashes were excluded. For each crash event, five non-crash events were randomly selected from the non-crash populations. Finally, in the dataset of real-time safety analysis, there were 1,951 crash and 9,444 non-crash events, and each was matched with the complete traffic and geometry information.

4.3 Methodology

4.3.1 Case-control Design

In the real-time crash analysis, the number of non-crash events greatly outnumbers that of crash events. For example, if a segment has 10 crashes in a year, the number of crash events is 10 (each one at five-minute intervals); on the other hand, the number of non-crash events is around 100,000. It would be impractical to put all the non-crash events in the model analysis, so a case-control design was adopted in this study: *n* crash events were selected from the population of crash events, and a sample of *5n* non-crash events was selected from the population of non-crash events.

The logistic regression is able to handle the case-control design because it can achieve a valid odds ratio from the estimated coefficients of independent variables in the case-control design

(Hosmer et al., 2013). Suppose *A* is a crash event, and *B* stands for an observation in the dataset of the real-time crash analysis that is selected from the whole population; the possibility that a selected observation is a crash event is *p(A|B)*, which is calculated as follows:

$$p(A|B) = \frac{p(A)p(B|A)}{p(A)p(B|A) + p(\overline{A})p(B|\overline{A})} \quad (4.1)$$

where $\overline{A}$ means an observation is not a crash event. From Equation (4.1), the ratio is as follows:

$$\frac{p(A|B)}{1-p(A|B)} = \frac{p(A)p(B|A)}{p(\overline{A})p(B|\overline{A})} \quad (4.2)$$

Suppose that $p(B|A)$ is the percentage of crash events that have been sampled (p_1) and $p(B|\overline{A})$ is the percentage of non-crash events that have been sampled (p_2). Equation (4.2) could be written as follows:

$$\frac{p(A|B)}{1-p(A|B)} = \frac{p(A)}{1-p(A)} \times \frac{p_1}{p_2} \quad (4.3)$$

In a logistic regression model without case-control design, the crash ratio is estimated using the following equation:

$$\log\left(\frac{p(A)}{1-p(A)}\right) = \beta_0 + \sum_{r=1}^{R} \beta_r x_r \quad (4.4)$$

where β_0 is the threshold, and β_r is the estimated coefficient of the r^{th} explanatory variables (x_r). Putting Equation (4.4) into Equation (4.3), the crash ratio under case-control design is as follows:

$$\log\left(\frac{p(A|B)}{1-p(A|B)}\right) = \ln\left(\frac{p_1}{p_2}\right) + \beta_0 + \sum_{r=1}^{R} \beta_r x_r = \beta_0^{'} + \sum_{r=1}^{R} \beta_r x_r \quad (4.5)$$

By comparing Equations (4.4) and (4.5), it can be found that the only difference between the logarithm of crash ratio under case-control design and that under non-case-control design is the intercept. Hence, in order to obtain the true intercept β_0, $\ln(p_1 / p_2)$ should be subtracted from $\beta_0^{'}$, which is estimated under case-control design. Both p_1 and p_2 are available, so the true crash ratio and then the true crash likelihood for each five-minute interval are ready to be calculated if the real-time crash analysis model is obtained.

4.3.2 Crash Prediction Models

In the hourly crash analysis, each segment has 24 observations in total. In the real-time safety analysis, a segment has several crash and non-crash events. The observations on the same segment might be correlated; meanwhile, a segment might have different crash potentials compared with other segments since there might be some uncaptured characteristics of each segment. Multilevel models were used to handle the two issues (Gelman & Hill, 2006).

For ADT-based total crash frequency estimation, a Bayesian Poisson-lognormal model was used. The Poisson-lognormal model has been widely used in crash frequency analyses to handle the over-dispersion problem (Lord & Mannering, 2010). For the AHT-based crash frequency prediction, a Bayesian multilevel Poisson-lognormal model was used. It was assumed that the observed crash frequency at time interval *t* on segment *i* (y_{ti}) had a Poisson distribution, whose mean was the expected crash frequency ($\boldsymbol{\lambda}_{ti}$):

$$y_{ti} \sim Poisson(\lambda_{ti}) \tag{4.6}$$

Individual level:

$$\log(\lambda_{ti}) = \beta_{0i} + \sum_{r=1}^{R} \beta_r x_{rti} + \mu_{ti} \tag{4.7}$$

Segment level:

$$\beta_{0i} \sim Normal(g_i, 1/\tau_2) \tag{4.8}$$

$$g_i = \gamma_0 + \sum_{q=1}^{Q} \gamma_q w_q + \varepsilon_i \tag{4.9}$$

where β_r is the regression coefficient of the r^{th} individual-level independent parameter (x_r), *R* is the total number of individual-level independent parameters, and μ_{ti} is the residual and was set to follow a normal distribution. β_{0i} is the intercept at the individual-level model; it was assumed to vary across segments and is conditioned on the geometric factor g_i. γ_0 is the intercept of segment level, γ_q is the coefficient of the q^{th} segment-level variable (w_q), *Q* is the total number of segment-level independent parameters, ε_i is the unexplained segment-level errors and is normally distributed with a mean of 0 and a deviation of τ_3. All γ_0, γ_q, and β_r were specified to be vague normal distributed priors: normal (0, 10^6). τ_1, τ_2, and τ_3 were specified to have gamma prior: gamma (0.001,0.001).

For the five-minute-based safety analysis under case-control design, a Bayesian multilevel logistic regression model was used. An observation at time interval *t* on segment *i* (y_{ti}) has a binary outcome, crash (y_{ti}=1) and non-crash (y_{ti}=0); their possibilities are p_{ti} (y_{ti}=1) and 1-p_{ti} (y_{ti}=0), respectively:

$$y_{ti} \sim Bernoulli(p_{ti}) \tag{4.10}$$

Individual level:

$$\log\left(\frac{p_{ti}}{1-p_{ti}}\right) = \beta_{0i} + \sum_{r=1}^{R} \beta_r x_{rti} \tag{4.11}$$

Segment level:

$$\beta_{0i} \sim Normal(g_i, 1/\tau_1) \quad (4.12)$$

$$g_i = \gamma_0 + \sum_{q=1}^{Q} \gamma_q w_q + \varepsilon_i \quad (4.13)$$

The variable definition of the Bayesian multilevel logistic regression model is similar to the Bayesian multilevel Poisson-lognormal model.

All three models, the Bayesian Poisson-lognormal, the Bayesian multilevel Poisson-lognormal, and the Bayesian multilevel logistic regression, were estimated in WinBUGS. For each model, three chains of 10,000 iterations were set up, and only the second half of the iterations were used in the final analysis to exclude the impact of the initial values (Gelman et al., 2014). For all parameters in the three Bayesian models, the trace plots of three chains appeared to have been stabilized, and the three chains were overlapping each other. This indicated that models were converged.

4.3.3 Model Comparison

After the three models were estimated, the total and hourly crash frequencies for each segment were calculated, and the true real-time crash likelihoods at five-minute intervals for each segment were also computed. Then, the predicted crash frequency and crash likelihoods were used to obtain the crash condition at three different levels: total, hourly, and five-minute intervals. To be more specific (Figure 4.2):

1. The predicted total crash frequency (based on ADT) was divided by 24 hours to obtain the hourly crash count and then divided by the number of five-minute intervals in the study period (884 days × 24 hours ×12 intervals) to obtain crash likelihoods at five-minute intervals;
2. The 24 hourly crash frequencies on each segment were all aggregated together to provide the total crash frequency of that segment, and they were also divided by the number of five-minute intervals in one-hour intervals throughout the study period (884 days × 12 intervals);
3. The conditional crash likelihoods at five-minute intervals under case-control design were first calculated and transferred to actual crash likelihood. Then, the actual crash likelihoods were aggregated into total crash frequencies and hourly crash frequencies.

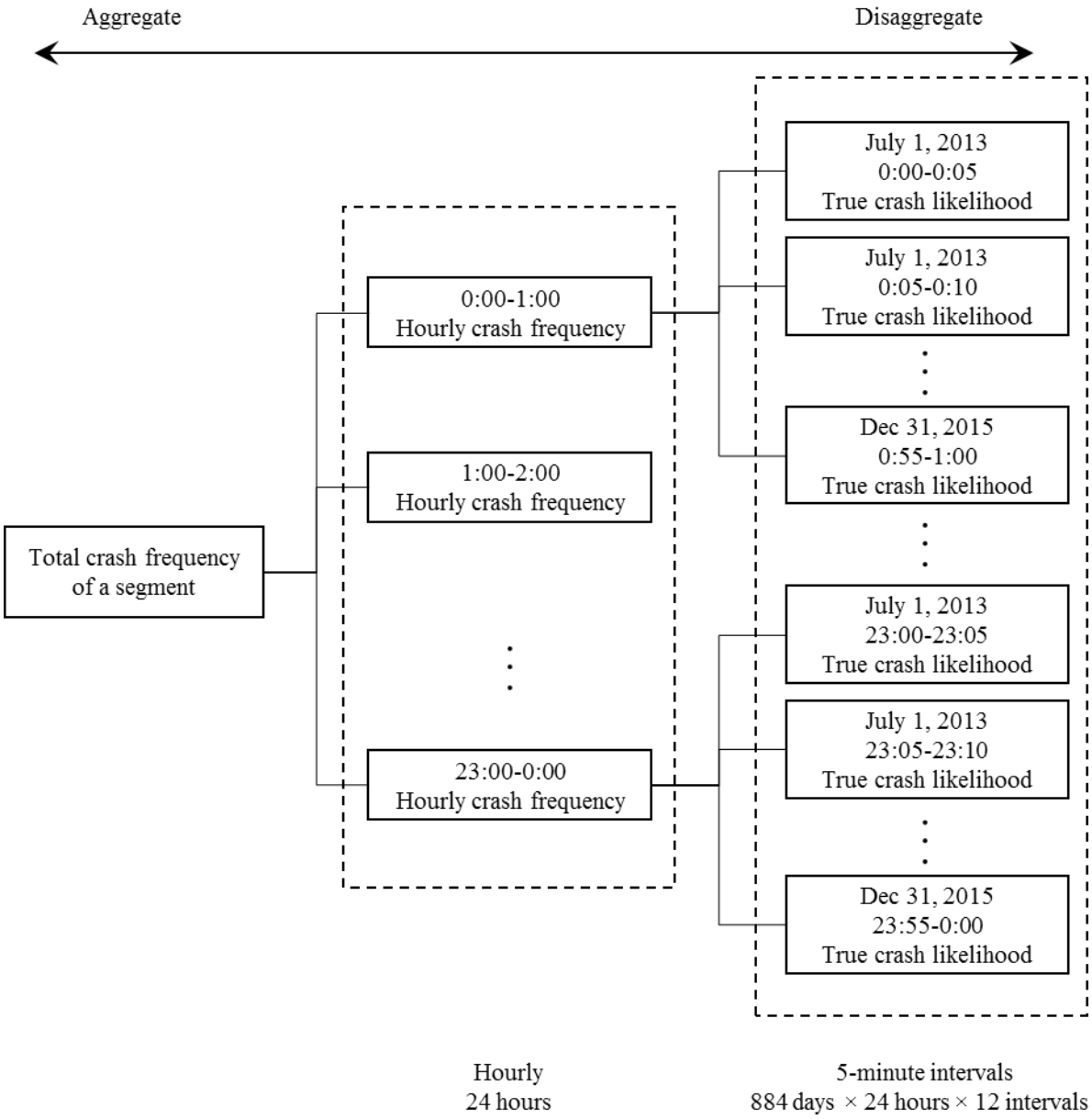

Figure 4.2 – Model results transformation.

After transformation, there were three estimated crash conditions, i.e., ADT-based, AHT-based, and five-minute-based, for each time level. Then, the estimated crash conditions were compared with the field crash conditions. For crash frequency comparison, mean absolute deviation (MAD) was used to estimate the consistency between estimated and true crash conditions,

$$\text{MAD} = \frac{\sum_{i=1}^{n} |y_i - \hat{y}_i|}{n} \quad (4.14)$$

where *n* is the number of total observations, y_i is the field crash frequency of the i^{th} observation, and $\hat{y}_i$ is the predicted crash frequency of the i^{th} observation.

With respect to the crash risk at five-minute intervals, the measurement area under the receiver operating characteristic (ROC) curve was adopted. The ROC is a standard for evaluating a model's ability to correctly assign an observation to the correct group (Hosmer et al., 2013). The curve plots the possibility of detecting true crash events and the possibility of detecting false crash events for an entire range of possible thresholds (from 0 to 1.0). The area under the ROC curve ranges from 0.5 to 1.0. A higher value indicates a better ability to discriminate crash from non-crash events.

One of the most important targets of real-time crash analysis is the identification of hazard conditions for ATM, such as RM. The segments and time period with high crash potentials are of great interest for ATM (Abdel-Aty et al., 2007). On the other hand, if a segment does not have any crashes over a very long period of time, there is no need to install ATM or to identify high crash risk. Hence, distinguishing crash events for the segments with high historical crash frequencies is better than doing so for all segments. For any hour-long interval (for example, 7:00 A.M. to 8:00 A.M.) throughout the study period (884 days), if a segment had more than one crash in that interval, this segment in this hour period was chosen to provide data at five-minute intervals for model comparison. In total, 1,065 crash events were filtered, and 5,325 non-crash events were randomly selected for ROC calculation.

4.4 Model Estimation and Comparison

4.4.1 Crash Prediction Model

Before model estimation, each independent variable alone was put into models to find out whether it had significant impact on safety at an 85% confidence interval. Then, after insignificant variables were deleted, Pearson correlation tests were conducted to evaluate the correlation between variables. When the correlation between a variable and volume was higher than 0.4, then this variable was excluded in the model building; when both of the variables were not volume, and their correlation coefficient was higher than 0.4, the variable that could provide a lower deviance information criterion (DIC) was chosen. The models' results are presented in Table 4.3.

Overall, the significant variables in the three models are similar. Four out of eight significant variables were common, and all common variables have the same signs. All significant variables in the ADT-based crash prediction model were included in the AHT-based crash prediction model. Meanwhile, except for one variable (speed), all significant variables in the five-minute-based safety analysis model could be found in the AHT-based crash prediction model. This indicates that the crash-contributing factors discovered by the three models were comparable.

Table 4.3 – Crash prediction model.

Definition	ADT-based			AHT-based			5-minute-based		
	Mean	Std.#	95% CI	Mean	Std.	95% CI	Mean	Std.	95% CI
Intercept	-0.74	2.09	(-5.29,3.66)	-4.84	0.94	(-6.66,-3.01)	-3.25	0.35	(-3.92, -2.58)
Log (volume per lane)	0.57	0.17	(0.25,0.92)	0.72	0.04	(0.65,0.79)	0.80	0.05	(0.71, 0.89)
Speed limit (mph)	-0.06	0.01	(-0.07,-0.04)	-0.04	0.01	(-0.06,-0.01)	--*	--*	--*
Speed (mph)	--*	--*	--*	--*	--*	--*	-0.05	0.00	(-0.06,-0.04)
Truck percentage	--*	--*	--*	1.54	0.54	(0.48,2.60)	2.57	0.33	(1.90,3.20)
Number of lanes (lane)	0.17	0.07	(0.04,0.30)	0.22	0.06	(0.10,0.34)	0.27	0.06	(0.15,0.38)
Segment length (10^3 ft)	0.14	0.01	(0.11,0.16)	0.15	0.01	(0.12,0.17)	0.16	0.01	(0.13,0.19)
Weaving segment	0.57	0.17	(0.24,0.90)	0.70	0.16	(0.39,1.01)	0.34	0.17	(0.03,0.68)
Diverge segment	--*	--*	--*	0.42	0.12	(0.18,0.65)	--*	--*	--*
std. of ε_i	N/A	N/A	N/A	0.43	0.20	(0.04,0.64)	0.23	0.18	(0.03,0.60)
DIC	1293.210			7712.350			5752.180		
Training ROC	N/A**			N/A			0.813		
Validation ROC	N/A			N/A			0.771		

Standard deviation

* Not significant

** Not available

The exposure variables, i.e., the logarithm of volume per lane, the number of lanes, and the segment length, were found to have significantly positive impacts on crashes in all three models. The higher the exposure variables, the higher the crash frequency and the higher the crash ratio. In addition to exposure variables, other traffic and geometric factors were also found to be significant. Speed had a negative impact on crash ratio in real time. High speed indicates that the traffic condition is smooth and there is no congestion, so the crash potential is low. The same negative relationship between speed and crashes has also been found by other researchers (Hossain & Muromachi, 2013a). Speed limit was negatively related to crash frequency. Segments with high speed limits are mainly in rural areas where there are fewer on- and off-ramps; hence, the number of lane changes because of on- and off-ramps is lower. Meanwhile, for the studied segments, the correlation coefficient between speed limit and median width was 0.59 and was significant at the 5% confidence interval. The large median width also enhanced the safety of segments (Park et al., 2016).

Truck percentage was not significant in the ADT-based crash prediction model. Truck percentage varies significantly at different hours of day (Pahukula et al., 2015). However, the ADT-based crash prediction model was not able to capture the variability and failed to link crash count with trucks. On the other hand, truck percentage was positively significant in both the AHT-based crash frequency and the five-minute-based crash analysis models. A higher truck percentage

results in a higher crash frequency and a higher crash ratio. The characteristics of passenger cars and trucks are different; for example, trucks travel with a lower speed than passenger cars (Johnson & Murray, 2010). A higher truck percentage implies more traffic turbulence and would increase crash potential.

Weaving segments are more dangerous than other types of segments. A weaving segment is a combination of a merge and a diverge segment. Hence, compared to other segments, weaving segments have more complicated traffic since vehicles merge, diverge, and cross each other over a short section (Wang et al., 2015a). Meanwhile, the high speed difference between weaving and non-weaving traffic might also be a reason that weaving segments have higher crash hazards (Pulugurtha & Bhatt, 2010). In the AHT-based crash prediction model, diverge segments had an increased crash frequency. Vehicles traveling from mainlines to off-ramps usually decelerate to adjust to the lower speed limit on off-ramps. If a vehicle decelerates significantly and its following vehicle does not react in time, a rear-end crash might happen. In this study, the crash characteristic confirms the interpretation. The rear-end crash percentage for diverge segments was 57.7%, which is significantly higher than for merge segments (40.0%), weaving segments (47.3%), and basic segments (39.2%).

With regard to the standard deviation of the segment-level error term, "std. of ε_i", it was statistically significant at the 5% confidence interval for both AHT-based and five-minute-based crash prediction models. It indicates that the between-segment variability was significant and implies that the multilevel model structure was appropriate.

4.4.2 Model Comparison Results

After three crash prediction models were obtained, they were compared. The comparison results are shown in Table 4.4.

Table 4.4 – Model comparison results.

From models \ To predict	MAD total crash frequency	MAD hourly crash frequency	ROC 5-minute crash likelihood
ADT-based model	1.060	0.473	0.599
AHT-based model	0.985	0.326	0.640
5-minute-based model	3.113	0.431	0.702

The results show that the AHT-based and five-minute-based model performed well in their own areas: the AHT-based model was the best model for estimating hourly crash frequency, and the 5-minute-based model was the best for distinguishing crash from non-crash events. On the other hand, the ADT-based model did not perform as well as the AHT-based model in predicting total crash frequency. Meanwhile, the ADT-based model performed the worst in predicting hourly crash frequency and crash likelihood at five-minute intervals. The result indicates that it is not appropriate to assume that traffic conditions are not diverse throughout the day or to suppose that the crash potential is evenly distributed.

The AHT-based crash prediction model performed the best in predicting total and hourly crash frequency. The studied expressways are mainly used for commuting; they have morning and evening traffic peak hours (see Figure 4.3). Volume is one of the most important crash-contributing factors; therefore, the field crash frequency also had two peaks, which were consistent with the traffic pattern. The hourly crash study was able to capture the traffic pattern better than the crash study based on ADT; additionally, the AHT-based model is better than the five-minute-based model because the aggregated hourly traffic largely excluded the impact of temporal turbulence.

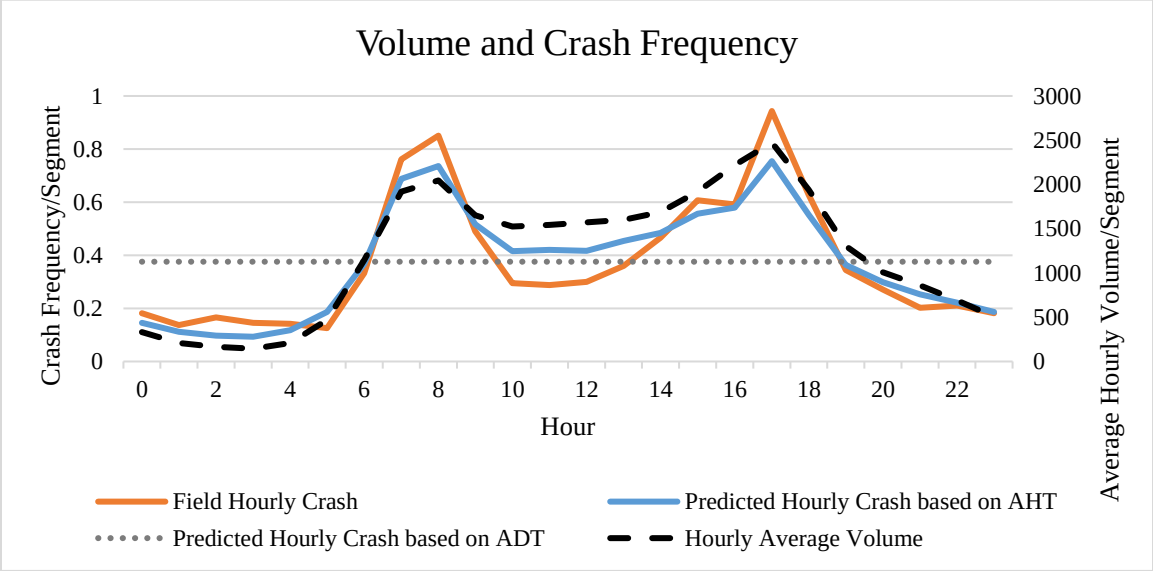

Figure 4.3 – Hourly volume and crash frequency.

The five-minute-based crash analysis model performed well in determining crash likelihood at five-minute intervals by providing a higher ROC. The ADT and AHT are aggregated traffic parameters; however, the occurrence of crashes could be attributed to temporal conditions. For example, a segment has a crash because of unexpected heavy traffic over several minutes during off-peak hours. The aggregated traffic factors might not be able to explain the occurrence of this crash, whereas the real-time crash analysis can.

4.5 Summary

The traffic safety studies based on ADT, AHT, and traffic at five-minute intervals have been widely and respectively explored by previous researchers. Nevertheless, there are not enough studies, which compare these three types of traffic safety analyses. This study first built three models: a Bayesian Poisson-lognormal model to estimate total crash frequency using ADT, a Bayesian multilevel Poisson-lognormal model to predict hourly crash frequency using AHT, and a Bayesian multilevel logistic regression model to estimate real-time crash risk under case-control design using traffic at five-minute intervals. Then, the models were compared to find their

ability to estimate crash frequency and crash likelihood at three levels (total, hourly, and five-minute intervals).

Overall, the significant variables in the three models were comparable. All estimation results of the three models showed that the logarithm of volume per lane, the number of lanes, the segment length, and the existence of a weaving segment were positively related to crash occurrence. On the other hand, some variables were not significant in all models; for example, truck percentage was significant only in the AHT-based and the five-minute-based crash model. The model comparison showed that the AHT-based crash prediction model performed best in estimating total and hourly crash frequency, and the five-minute-based crash prediction model was the best in distinguishing crash events for the segments with high crash potential. Additionally, it was found that the five-minute-based crash prediction model was the worst in estimating total crash frequency, and the ADT-based crash prediction model was the worst in predicting both hourly crash frequency and crash likelihood at five-minute intervals. It is recommended that different time intervals should be used in different situations: if researchers focus on long-term traffic safety, crash prediction models based on AHT are better than those based on ADT or traffic at five-minute intervals; if researchers intend to distinguish crash hazardous conditions and further apply ATM to improve traffic safety, the real-time crash analysis is better.

In sum, this chapter has found that the existence of a weaving segment would significantly increase crash potential. Hence, in order to improve the safety of the expressway system, the weaving segments should be the main focus. Meanwhile, the chapter proposed that real-time crash analysis could facilitate ATM to improve traffic safety, so real-time crash analysis for weaving segments should be explored.

5 Real-time Safety Analysis for Weaving Segments

5.1 Introduction

In urban areas, the demand of exiting and entering expressway traffic is high. Hence, more on- and off-ramps are needed than in rural areas. The dense on- and off-ramps might result in limited spacing between them. When an on-ramp is closely followed by an off-ramp and the two are connected by auxiliary lane(s), a weaving segment is formed. Weaving is generally defined as the crossing of two or more traffic streams traveling in a same direction along a significant length of highway without the aid of traffic devices (except for guide signs) (National Research Council, 2010). Normally, there are three types of movement in weaving segments: mainline-to-mainline, mainline-to-ramp, and ramp-to-mainline. There also might be some ramp-to-ramp traffic; however, this type of traffic is not frequent since a traveler is not very likely to pay a toll fee and just travel a short distance (normally less than 1 mile). Hence, ramp-to-ramp traffic is not considered. The three types of main traffic movements are shown in Figure 5.1.

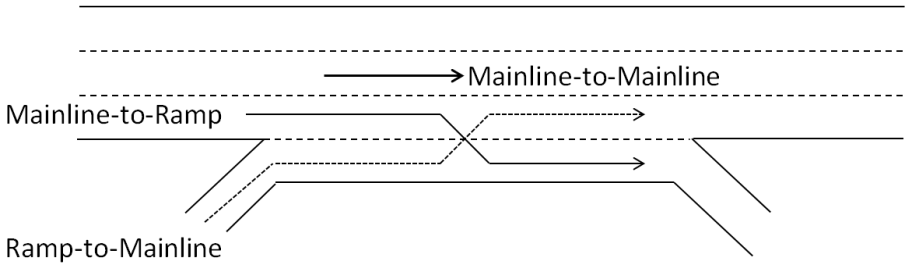

Figure 5.1 – Weaving segment traffic movements.

Traffic conditions in weaving segments are complicated because on-ramp and off-ramp vehicles have to compete for lane-changing opportunities in a limited distance. Meanwhile, low-speed entering vehicles need to accelerate in order to join mainline traffic, and exiting vehicles have to decelerate in order to adjust to the lower speed limits of off-ramps. These frequent lane-changing, acceleration, and deceleration maneuvers might result in an increased crash risk in weaving segments. As for a congested weaving segment, these maneuvers might be more intense, and the safety concerns of the congested weaving segment are more severe than other segments.

The occurrence of crashes in weaving segments can bring about serious results. On-ramp vehicles might not be able to get on expressways and may have to change their routes. Off-ramp traffic may have difficulty getting off mainlines and may queue up on mainlines. Moreover, if crashes cannot be cleared in time, the queue may block all traffic, both non-weaving and weaving. Then the capacity and level of service of weaving segments will be reduced significantly. Hence, understanding the crash mechanisms of weaving segments and finding potential solutions to mitigate crash risks are significantly important.

This chapter focuses on finding crash mechanisms of weaving segments by conducting a real-time safety analysis. In total, three types of explanatory parameters were considered in the model building. They were traffic, geometry, and weather explanatory variables. Of these, traffic explanatory variables are essential, and traffic turbulence is one of the most important contributing crash factors. The geometric characteristics, e.g., segment length and number of lanes involved in weaving, are more site-specific for weaving segments. Exploring the connection between geometric characteristics and crash would be helpful in finding hazardous weaving segments. Additionally, weather factors might also be important. Severe weather, e.g., rain, makes vehicles in weaving segments vulnerable to frequent lane-changing, deceleration, and acceleration maneuvers.

5.2 Methodology

A logistic regression model was built to quantify the impact of contributing factors on crash occurrence. Suppose an event, which is the i^{th} observation, has binary outcomes: crash (y_i=1) or non-crash (y_i=0). The possibilities for these two outcomes are p_i (y_i=1) and 1-p_i (y_i =0), respectively. The models are as follows:

$$y_i \sim Bernoulli(p_i) \tag{5.1}$$

$$\log it(p_i) = \beta_0 + \sum_{r=1}^{R} \beta_r x_{ri} \tag{5.2}$$

where y_i follows a Bernoulli distribution whose success probability is p_i, β_o is the intercept, β_r is the regression coefficient of predictor x_{ri}, and x_{ri} is the r^{th} explanatory variable for the i^{th} observation, e.g., volume.

This project implemented the k-fold cross-validation method to evaluate the prediction accuracy of the real-time crash risk model. The k-fold cross-validation method is able to minimize the bias caused by the random sampling of the training and validation data samples (Olson & Delen, 2008). In the k-fold cross-validation, the complete dataset is randomly divided into *k* mutually exclusive subsamples, each subsample having approximately equal sample size. The model is trained and tested *k* times. For each attempt, a subsample acts as the validation data for testing the model, and the remaining *k*-1 subsamples are used as training data. Each of the *k* subsamples is used exactly once as the validation data, so the cross-validation process is repeated *k* times in total. Then the *k* results from the *k* validation folds are combined to provide a single estimation of model performance. In this study, a 10-folder cross validation was adopted.

Crashes are rare events, so the number of non-crash events is much larger than that of crash events. However, it is not practical to put millions of non-crash events in safety analysis. Thus, this study applies the case-control design to provide a valid estimation of a variable's impact on crash odds ratios and also on conditional crash risks (Vittinghoff et al., 2011).

5.3 Data Collection

Data from 16 weaving segments on SR 408 were collected since the number of weaving segments on SR 408 is much higher than on the other two studied expressways. Four datasets were collected and processed: crash, traffic, weather, and geometry. The study period was from July 2013 to April 2015. However, due to the absence of traffic data in April 2014, only 21 months' worth of data were used.

The crash data were from the S4A, including crash time, location, type, severity, etc. The traffic data were provided by the MVDS, containing traffic count, lane occupancy, and speed per lane per minute interval. As for the weather data, it was collected from the NCDC, which recorded the weather for the Orlando Executive Airport (ORL). ORL is less than 0.5 miles north of the middle of SR 408. The geometric data, e.g., weaving segment length, were manually collected using the ArcGIS map.

The crash events were the conditions 5-10 minutes before crashes (Wang et al., 2015b); the non-crash events were the conditions that neither resulted in a crash nor were impacted by a crash. In this study, the non-crash conditions were more than five hours before and after crashes. The non-crash events were also based on five-minute intervals. The variables used in the real-time safety analysis are listed in Table 5.1.

Table 5.1 – List of variables.

Variables*	Definition
Bm_spd	Average speed at the beginning of weaving segments (mile/h)
Em_spd	Average speed at the end of weaving segments (mile/h)
Spd_{dif}	Speed difference. Spd_{dif}=0 if Bm_spd is lower than Em_spd; otherwise Spd_{dif}= Bm_spd- Em_spd
Vehcnt	Total traffic count in the weaving segment (vehicles)
VR	Weaving volume ratio, weaving volume over the total traffic count (%)
N_{WL}	Lanes from which weaving maneuvers may be made with one or no lane changes (lane)
LC_{RF}	Minimum number of lane changes that must be made by a single weaving vehicle moving from the on-ramp to the expressway (lane)
LC_{FR}	Minimum number of lane changes that must be made by a single weaving vehicle moving from the expressway to off-ramp (lane)
LC	Weaving configuration, when LC_{RF}=LC_{FR}=1, LC=0; otherwise 1
L_{max}	Weaving influence length (1000 feet) #
Wet	1=if the pavement surface condition is wet; 0=otherwise

* All traffic data are calculated in a five-minute interval and in the weaving segment
# $L_{max}=5728(1+VR)^{1.6}-1566N_{WL}$ (HCM, 2010)

5.4 Crash Prediction Model

One hundred and sixty-five crashes were identified in the weaving segments on SR 408 during the study period, among which 125 crashes had complete traffic and weather information. For each crash event, 20 non-crash events were randomly selected from the non-crash-event population.

The correlations between independent variables were checked to exclude highly correlated variables. Then, the PROC LOGISTIC procedure in the Statistical Analysis System (SAS) was used to obtain the real-time crash risk estimation model. SAS is a commercial software for data processing, advanced analytics, predictive analytics, etc. The ten-folder cross-validation method was used to validate model performance. The model's results are presented in Table 5.2.

Table 5.2 – Real-time crash estimation model for weaving segments.

Variables	Definition	Mean	Std.	p-value
Intercept	Intercept	-7.86	0.79	0.00
Spd_{dif}	Speed difference	0.11	0.03	0.00
Log(Vehcnt)	Logarithm of total traffic count	0.65	0.12	0.00
LC	Weaving configuration	0.57	0.20	0.01
L_{max}	Weaving influence length	0.21	0.07	0.00
Wet	Pavement surface condition	1.22	0.24	0.00
Training ROC			0.716	
Validation ROC			0.704	

The performance of a logistic regression model was measured by ROC (Hosmer et al., 2013). The value of ROC is between 0.5 and 1.0. A higher ROC value indicates a better ability to discriminate crash and non-crash events. Both the training and validation ROC of the real-time crash estimation model in Table 5.2 were more than 0.7. This indicates that the model provided acceptable discrimination between crash and non-crash events (Hosmer et al., 2013).

The speed difference between the beginning and the end of the weaving segment was found to be positively related to crash risk. This result is consistent with previous studies (Hossain & Muromachi, 2010). As for the configuration (LC), when the minimum number of lane changes for on-ramp or off-ramp vehicles is zero, the crash risk is increased. A similar finding was also presented by other researchers (Liu et al., 2009). A longer weaving influence length indicates more intense weaving maneuvers, thus a higher crash risk. Vehicles on wet pavement surface have a higher probability of losing control than on dry pavement surface and also need longer braking distance. Thus, the wet pavement surface raises crash risk.

The conditional crash risk (p) based on case-control design can be obtained from Table 5.2 by using the following function,

$$p = \frac{\exp(-7.86 + 0.11Spd_{dif} + 0.65\log(vehcnt) + 0.57LC + 0.21L_{\max} + 1.22Wet)}{1 + \exp(-7.86 + 0.11Spd_{dif} + 0.65\log(vehcnt) + 0.57LC + 0.21L_{\max} + 1.22Wet)} \quad (5.3)$$

But what needs to be kept in mind is that the crash estimation model for the weaving segment was based on a case-control design. The true crash risk cannot be obtained, but the crash odds ratio (*OR*) between two conditions (Condition 1 and Condition 2) can be obtained using the following function:

$$OR = \frac{Crash\ Odds_2}{Crash\ Odd_1} = \exp\{0.11(Spd_{dif\,2} - Spd_{dif\,1}) + 0.65[\log(vehcnt_2) - \log(vehcnt_1)] + 0.57(LC_2 - LC_1) + 0.21(L_{\max 2} - L_{\max 1}) + 1.22(Wet_2 - Wet_1)\} \quad (5.4)$$

If *OR* is higher than 1, it means Condition 2 is more dangerous than Condition 1; if *OR* is 1, it means the safety of Condition 2 is the same as the safety of Condition 1; if *OR* is less than 1, it means Condition 2 is safer than Condition 1.

When an ATM strategy is used, the crash odds ratio can be obtained if the values of traffic, geometry, and weather parameters are given. Then, the Equation (5-4) can be used to verify whether the ATM has a positive impact on safety.

5.5 Summary

The safety of weaving segments is a big concern since vehicles change lanes, weave, decelerate, and accelerate in a limited space. In order to improve the safety of a weaving segment, the first step is understanding the crash-contributing factors in weaving segments. This chapter applied a real-time safety analysis for weaving segments. The result showed that the logarithm of volume, speed difference between the beginning and end of a weaving segment, weaving influence length, configuration, and wet roadway surface condition had a positive impact on crash risk. An increase in these parameters would significantly increase crash potential.

Consequently, based on the real-time crash prediction model, a formulation was built. It could be used to test the crash odds ratio under different conditions. Using the formulation, the impact of ATM on weaving segment safety can be calculated.

6 Microsimulation Network Building

6.1 Study Segment Identification

6.1.1 Key expressway

As stated in Chapter 1, three major expressways (SR 408, SR 417, and SR 528) in Central Florida were selected as study subjects. Among these three expressways, SR 408 was selected to build a VISSIM network for potential safety improvement. There were three reasons why SR 408 was chosen:

1. SR 408 carried the heaviest daily traffic. By using MVDS traffic data, traffic volume on the expressways could be examined at a more microscopic level. As illustrated in Figure 6.1 and Appendix B, the spatio-temporal characteristics of hourly traffic volume on the mainline could be easily captured, and they confirm that westbound SR 408 serves the heaviest traffic among the studied subjects;
2. SR 408 experienced serious congestion most frequently. Congested segments were identified by measuring occupancy, which is defined as the percent of time a point on the road is occupied by vehicles (Hall, 1996) and was recorded by MVDS every one minute. The higher occupancy value indicates more congestion. This project divided occupancy into three categories: when a segment's occupancy is lower than 15%, there is no congestion; when its occupancy is higher than 15% and less than 25%, it is moderately congested; when its occupancy is higher than 25%, it is highly congested. Figure 6.2 and Appendix C plot the weekday occupancy for the three expressways in August 2015 and implied that westbound SR 408 was more congested than eastbound SR 408, and also more congested than any directions of the other two expressways;
3. SR 408 had more traffic crashes than other expressways. SR 408 serves as a backbone of the Central Florida Expressway system. Meanwhile, it passes through downtown Orlando, and provides access not only to residential areas, but also to commercial, retail, and government offices in the city center. Therefore, the ramp density and volume of SR 408 is much higher than the other two expressways. The higher ramp density and higher volume resulted in higher crash risk (Park et al., 2010). Table 3.2 compares the number of crashes on three expressways. It verifies that SR 408 was the expressway with the most crashes from 2013 to 2015. Meanwhile, the crash rate (crash per mile) of SR 408 is more than twice as high as that of the other two expressways.

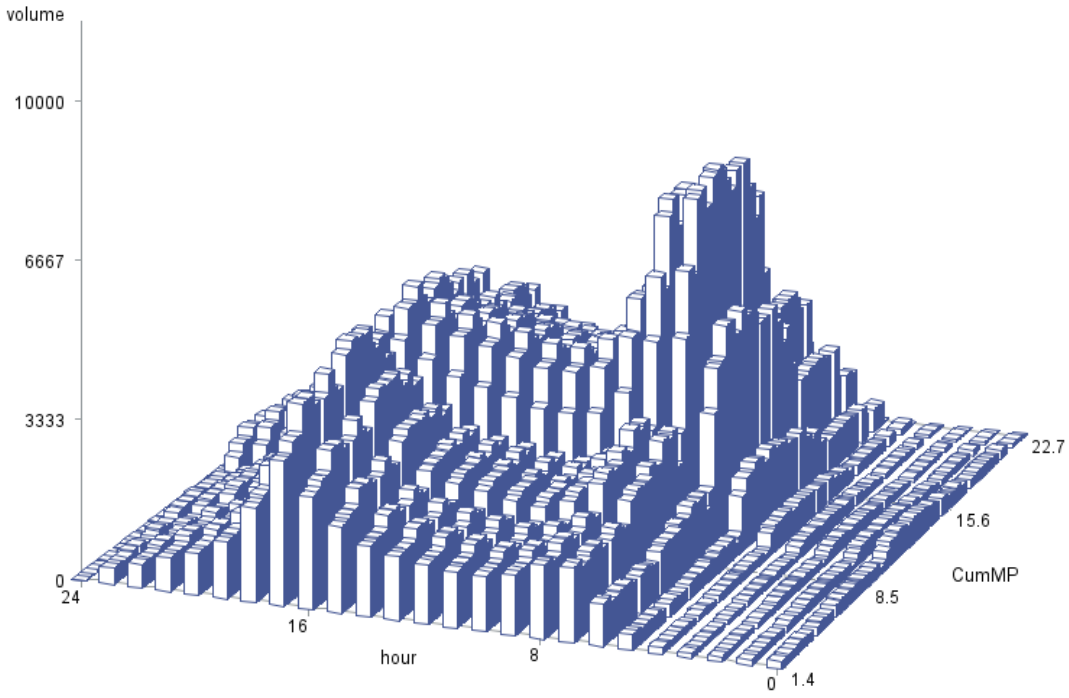

Figure 6.1 – Weekday hourly volume of SR 408 westbound in August 2015.

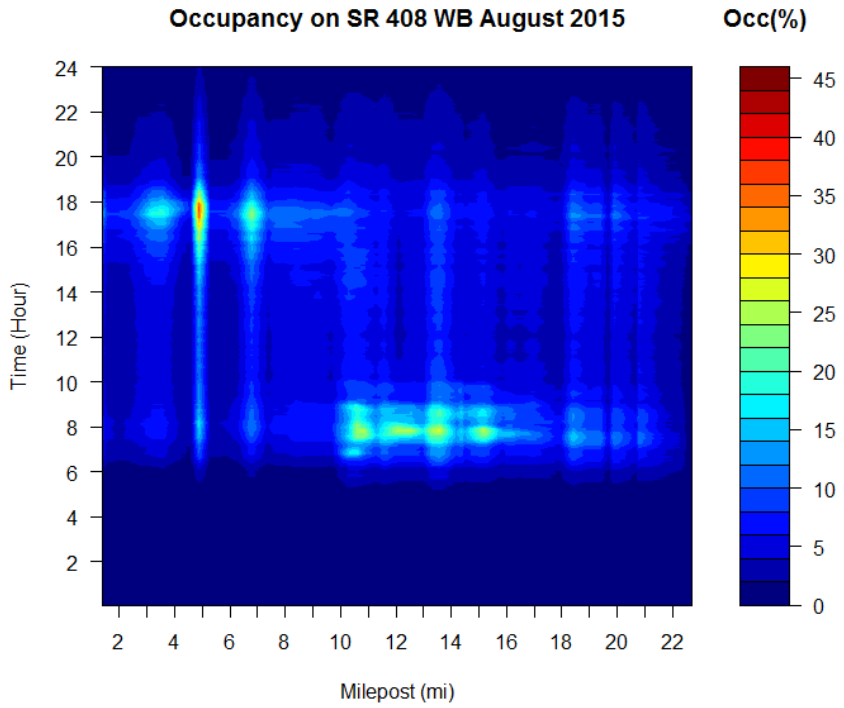

Figure 6.2 – Weekday occupancy of SR 408 westbound.

6.1.2 Key segment

After selecting SR 408, the next step was deciding the key study segment. Based on the weekday occupancy of SR 408 in August 2015 (see Figure 6.2 and Appendix C-1), the congestion conditions of SR 408 can be summarized as follows:

1. The congestion on the westbound lanes was more severe than that on the eastbound lanes, and the most congested period of the westbound segment was around 7:00 A.M. to 9:00 A.M.
2. The most congested segment is between milepost 10 and 16. To select a key segment for potential safety improvement, the congested MP 12.1 to MP 13.3 segment on the westbound lanes was chosen. This segment contains a weaving segment that was identified in Chapter 4 as having more crashes than other segment types. The length of the weaving segment is only about 1,400 feet in which diverging and merging maneuvers cannot be separately conducted.
3. The congestion intensity changed by time. When approaching peak hours, the congestion intensity gradually increased. Once the peak time passed, the congestion became less severe. Therefore, in addition to studying the congestion period, there was also a need to study the time before and after the congestion period. Hence, one and half hours before and after the peak hours were also analyzed. The study period was from 6:30 A.M. to 10:30 A.M.

The weekday traffic data from August 2015 was selected to represent the average traffic condition of the whole year. The main traffic on SR 408 is commuting traffic, so the weekday

traffic condition on SR 408 does not vary considerably across months. Figure 6.3 displays the 6:30 A.M. to 10:30 A.M. weekday average hourly volumes of a section whose milepost is 12.6 on westbound of SR 408. The average hourly volume over 12 months in 2015 was 6,521 vehicles, and the standard deviation was 273 vehicles. The weekday hourly volume in August was 6,586 vehicles, which was almost the same as the average hourly volume over a year.

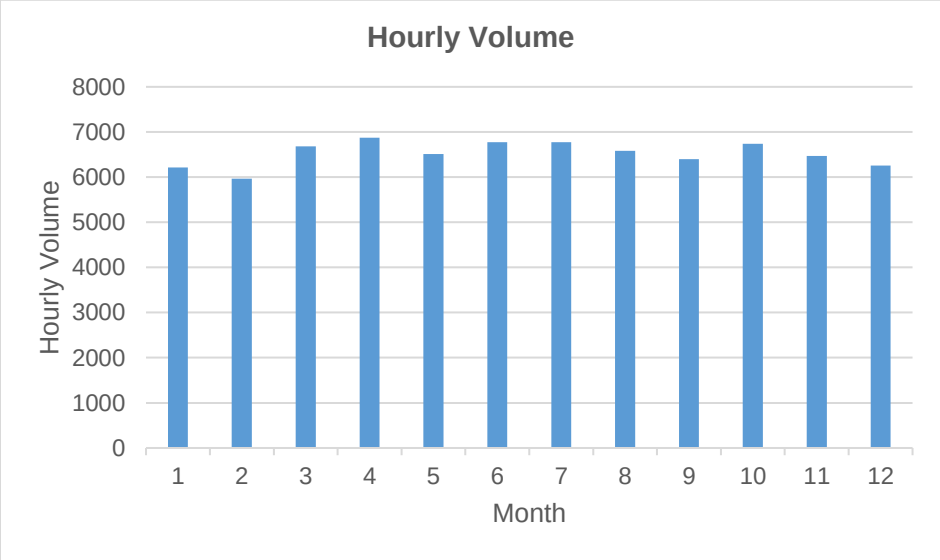

Figure 6.3 – Weekday hourly volume in 2015.

6.2 Network Coding

The two basic components of the VISSIM roadway network are links and connectors. The links represent roadway segments and are connected to other links by connectors. Vehicles cannot travel from one link to another without connectors attached. For each link, several properties must be specified: (1) number of lanes for the segment; (2) behavior type—there are six types of behavior in total, and freeway (free lane selection) was selected in this project; (3) lane width, set as 12.0 feet; and (4) gradient, set as 0% since the study segment is flat. Curvatures of the studied segment were coded through adjusting the shape of links and connectors to follow the roadway shapes in the background Bing maps, which is toggled in VISSIM. Finally, the coded expressway segment could accurately represent the geometric characteristics of the studied expressway segment. Figure 6.4 displays the coded segment with the background map. Links are blue and connectors are red.

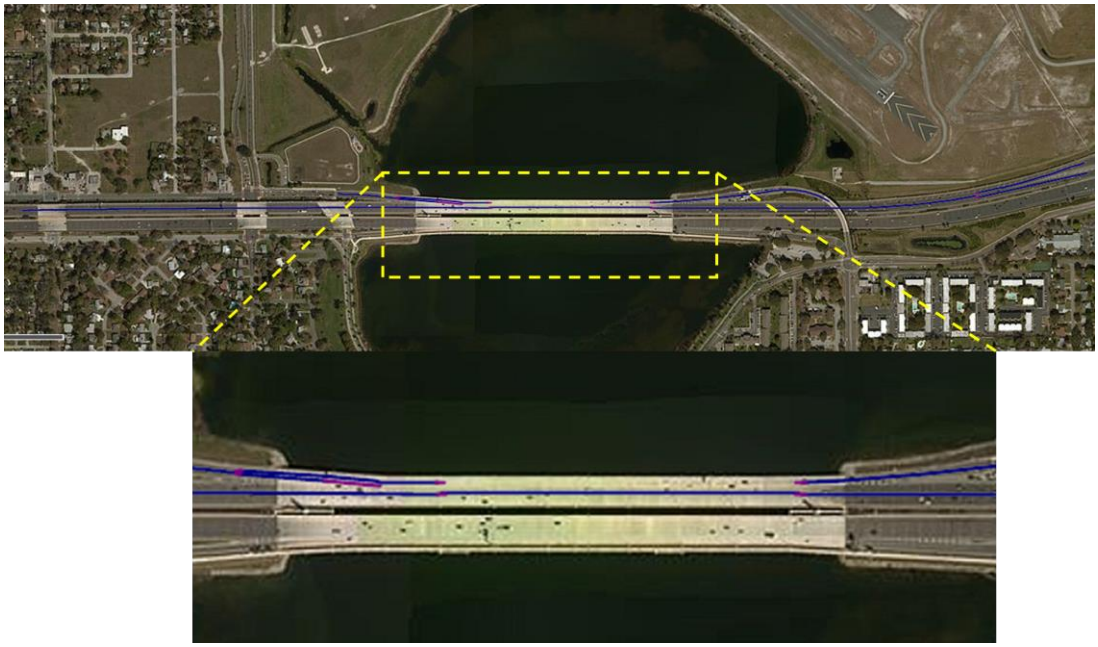

Figure 6.4 – Coded freeway section with background image.

In order to obtain traffic information from the VISSIM network, data collection points were added in the simulation network. They were installed at the exact location of field MVDS detectors to capture simulated traffic data. A data collection point recorded the time when the front of a car reaches the point, the time when the rear of a car leaves the point, vehicle type, speed, acceleration, etc. One data collection point can only catch traffic information for one lane. Hence, if a segment has several lanes, multiple data collection points should be placed on that segment. Figure 6.5 shows partial coded data collection points. The first letter of the name stands for lane type: Mainline (m), Ramp (r), Toll Plaza Express (e), and Toll Plaza Cash (c). The number following the lane type is milepost. The numbers in parentheses are lane id. The innermost lane's id is 1. By coding data collection points in this way, the simulation output data can be easily processed.

Data Collection Points

Select layout... <Single List>

Count: 23	No	Name
7	115	m12.6(1)
8	116	m12.6(2)
9	117	m12.6(3)
10	118	m12.6(4)
11	119	m12.6(5)
12	120	r12.6(6)
13	121	r12.6(7)
14	122	m12.1(5)
15	123	m12.1(1)
16	124	m12.1(2)

Figure 6.5 – Data collection points in VISSIM.

6.3 Field Traffic Data Input

In addition to the network geometric characteristics, links, connectors, and data collection points, traffic data are needed, i.e., volume, vehicle composition, and speed distribution.

The simulation period was from 6:30 A.M. to 10:30 A.M. In this simulation period, volumes on four Thursdays in August 2015 have been obtained from MVDS detectors, which provided traffic count at one-minute intervals. Then, these raw traffic data were further aggregated to 15 minutes to provide traffic inputs in VISSIM.

Meanwhile, vehicle composition information was an important traffic input as well. In VISSIM, there are two main vehicle types: passenger car (PC) and heavy goods vehicle (HGV). The composition information was also obtained by using MVDS data, which recognized the length of passing vehicles. The lengths of vehicles in Groups 3 and 4 were greater than 24 feet. These vehicles were considered as HGV in VISSIM. The percentages of PC and HGV were captured at 15-minute intervals.

Another traffic parameter is desired speed distribution. Desired speed is defined as drivers' speed when they are not hindered by other vehicles or network objects (PTV Group, 2013). The desired speed information was difficult to capture because there were always several vehicles on studied segments, and vehicles were always hindered by other vehicles. Nevertheless, a substitute of desired speed could be obtained by analyzing the speed of vehicles during daytime off-peak hours. During off-peak hours, the possibility of a vehicle constrained by other vehicles was low, and the vehicles were more likely to travel at their desired speed.

Figure 6.6 displays the traffic condition of milepost 13.0 on the westbound of SR 408. In this figure, the average 5-min volume of Thursdays in August 2015 illustrates that the traffic volume from 11:00 A.M. to 1:00 P.M. was the lowest during the daytime. Hence, the speed data during 11:00 A.M. to 1:00 P.M. on Thursdays in August 2015 were chosen to provide desired speed distribution information.

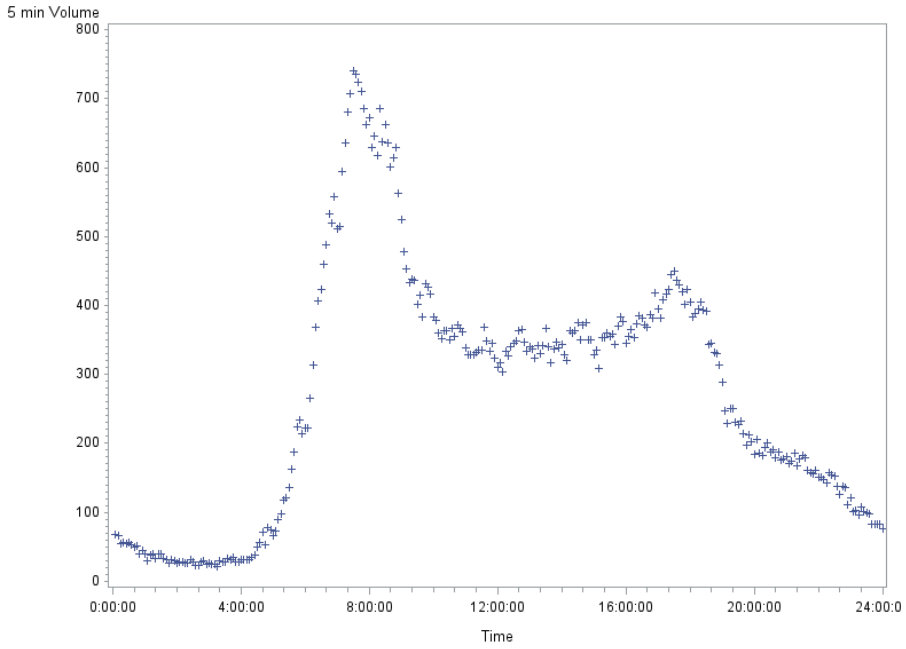

Figure 6.6 – Average 5-min volume on Thursdays in August 2015.

After deciding the time period for collecting desired speed distribution data, field cumulative speed distributions were formulated with the MVDS speed data by different lane types: mainline, on-ramp, off-ramp, toll plaza express lane, and toll plaza cash lane. Figure 6-7 displays an example of the speed distribution for the mainline.

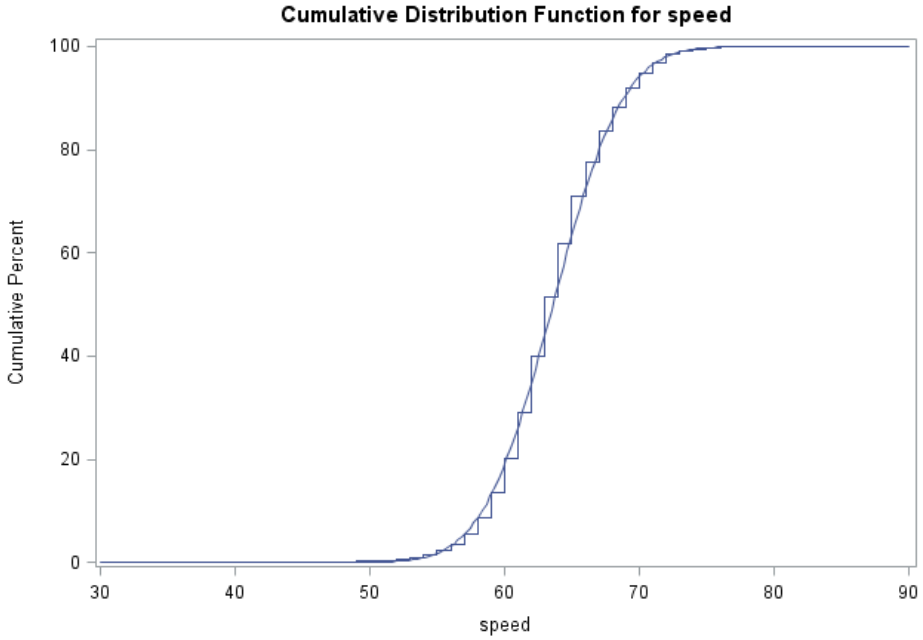

Figure 6.7 – Cumulative speed distribution for mainline.

The MVDS data provided the average speed for all vehicle types, but did not provide speed for different vehicle types (i.e., PC and HGV). Nevertheless, VISSIM had to specify desired speed distributions for different vehicle types. Therefore, one assumption was made to facilitate the calculation of desired speed distributions: the average speed of PC was 8.1 mph higher than that of HGV (Johnson & Murray, 2010).

From the MVDS data, it can be found that the average HGV percentage of the study segment was about 10%. Supposing x is the speed of PC, the speed for HGV is equal to (x-8.1), and the average speed provided by MVDS is y. Then,

$$0.9\,x+0.1\,(x-8.1)=y \qquad \textbf{(6.1)}$$

From Equation (6.1), the passenger car speed was found to be about y+0.8, and the HGV speed was around y-7.3. Then the desired speed distribution of PC and HGV were acquired separately. Figure 6.8 gives an example of the mainline desired speed distribution for PC and HGV.

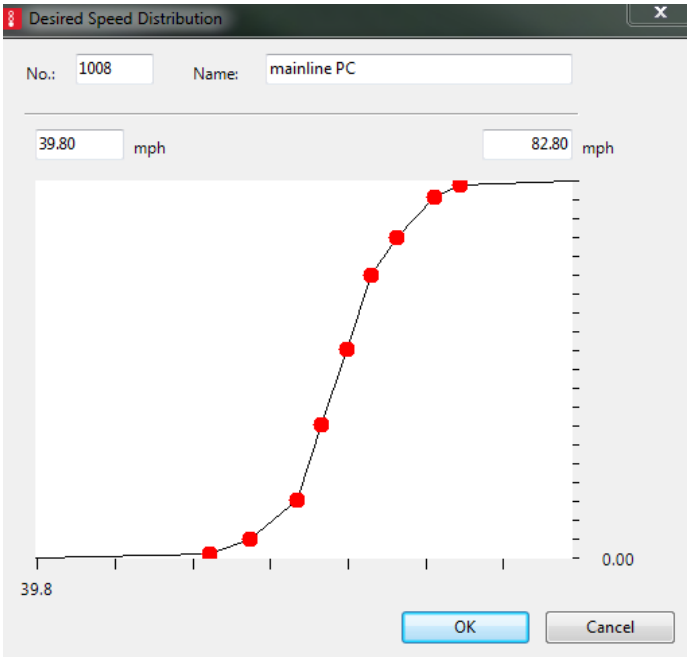

(a) Desired speed distribution of PC

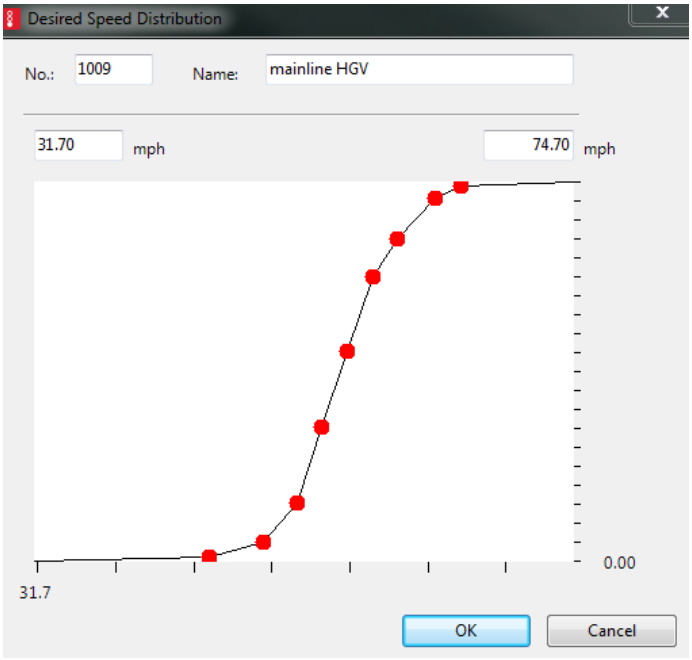

(b) Desired speed distribution of HGV

Figure 6.8 – Mainline desired speed distribution of (a) PC and (b) HGV.

6.4 VISSIM Network Calibration and Validation

After the required VISSIM elements were set up, network calibration and validation were conducted. If there was a big difference between field traffic and VISSIM simulated traffic, the traffic condition in the simulation network would fail to represent the real network, and the tests based on simulation would not be not valid. Hence, calibrating and validating VISSIM traffic are among the most important and basic tasks in the process of building a simulation network. Only after a simulation network is satisfactorily calibrated and validated can the network be used for further application, such as safety improvement and efficiency test.

Geoffrey E. Havers (GEH) was calculated to calibrate the VISSIM simulation network by comparing simulated volume and field volume (Dowling et al., 2004). The definition of GEH is as follows:

$$GEH = \sqrt{\frac{(E-V)^2}{(E+V)/2}} \tag{6.2}$$

where E is simulated volume (vehicles per hour) and V is field volume (vehicles per hour). If more than 85% of the measurement locations' GEH values are less than 5, then the simulated volume would accurately reflect the field volume (Yu & Abdel-Aty, 2014).

For the network validation, the absolute speed difference between the simulated traffic and field traffic was taken as validation index. According to Nezamuddin et al. (2011), the absolute value of speed difference should be within 5.0 mph for 85% of the checkpoints.

Previous studies have found that the desired lane change distance (DLCD) for weaving segments in VISSIM was different from other segments and was also different from the default value of VISSIM (200 meters) (Koppula, 2002; Woody, 2006). Hence, the DLCD was adjusted to get a better validation result. It was set from 200 to 1000 meters, with an increment of 100 meters. The result showed that the VISSIM network was better calibrated and validated when DCLD was 700 meters.

After excluding 30 minutes of VISSIM warm-up time and 30 minutes of cool-down time, a total of 180 minutes of VISSIM data were put into use. Table 6.1 shows an example of GEH values for the ramp and mainline of MP 13.0, which is located at the beginning of a weaving segment. The table shows that the section was well calibrated. Only three out of 24 observations' GEHs were higher than 5.0, among which two observations' GEHs were just 0.34 higher than 5.0.

In this simulation run, 94.4% observations' GEH were less than 5.0. The difference between the sum of all link simulation flows and that of all link field flows is 3,616, which was only 1.50% of the sum of all link field flows. Meanwhile, the average GEH for the sum of all link counts was 2.05. Furthermore, a total of 10 simulation runs with different random seeds has been conducted to confirm the calibration result. Ten simulation runs' results showed that the average GEH was 1.97 and 96.4% observations' GEHs were less than 5. Hence, the VISSIM calibration target was reached.

Table 6.1 – Sample of GEH values for calibration.

Time	MP 13.0 Ramp				MP 13.0 Mainline			
Interval	F_ Vol*	V_ Vol#	Abs(Dif)	GEH	F_ Vol	V_ Vol	Abs(Dif)	GEH
3	518	528	10	0.44	6461	6380	81	1.01
4	658	528	130	5.34	7862	7848	14	0.16
5	642	608	34	1.36	8043	8012	31	0.35
4	554	472	82	3.62	7526	6784	742	8.77
5	504	552	48	2.09	7069	7056	13	0.15
6	540	440	100	4.52	7405	7156	249	2.92
7	514	428	86	3.96	6894	7028	134	1.61
8	448	464	16	0.75	6417	6284	133	1.67
9	434	420	14	0.68	5021	5160	139	1.95
10	397	372	25	1.27	4711	4632	79	1.16
11	450	492	42	1.94	4472	4484	12	0.18
12	395	352	43	2.22	4511	4600	89	1.32
13	518	528	10	0.44	6461	6380	81	1.01
14	658	528	130	5.34	7862	7848	14	0.16
Average	642	608	34	1.36	8043	8012	31	0.35

* Field volume

VISSIM simulation volume

Once it was confirmed that the VISSIM network was well calibrated, the validation was done based on speed comparisons between VISSIM and field traffic data at 15-minute intervals. Table 6.2 displays an example for error of speeds at three locations, including two mainline sections and one toll plaza cash section. Results shown in the table prove that simulated speeds were satisfactorily validated and that the errors are within acceptable ranges.

Table 6.2 – Speed differences for validation.

Time Interval	MP	Type	F_speed*	V_speed#	Abs(speed_dif)*
3	12.6	Mainline	61.91	55.71	6.20
4	12.6	Mainline	56.85	47.78	9.07
5	12.6	Mainline	40.56	41.38	0.82
6	12.6	Mainline	37.46	40.94	3.48
7	12.6	Mainline	48.41	45.76	2.65
8	12.6	Mainline	54.65	53.72	0.94
9	12.6	Mainline	51.24	51.53	0.29
10	12.6	Mainline	54.4	56.22	1.82
11	12.6	Mainline	62.31	59.81	2.50
12	12.6	Mainline	62.25	59.78	2.48
13	12.6	Mainline	58.05	60.63	2.58
14	12.6	Mainline	57.34	60.42	3.08
3	13.0	Mainline	62.51	59.95	2.57
4	13.0	Mainline	59.07	58.57	0.50
5	13.0	Mainline	53.03	52.25	0.78
6	13.0	Mainline	49.65	51.3	1.65
7	13.0	Mainline	54.93	59.5	4.57
8	13.0	Mainline	61.02	60.28	0.74
9	13.0	Mainline	55.42	60.64	5.22
10	13.0	Mainline	60.89	60.84	0.05
11	13.0	Mainline	63.76	60.66	3.10
12	13.0	Mainline	63.16	61.4	1.77
13	13.0	Mainline	62.03	61.3	0.73
14	13.0	Mainline	62.42	61.05	1.37

* Absolute value of speed difference

Additionally, nine more runs were carried out to confirm the validation result. Overall, 86.46% observations' absolute values of speed difference were less than 5.0 mph. Therefore, the VISSIM network was successfully validated.

6.5 Summary

This project aims to improve the safety of a key segment. Both congestion and complicated geometric design may increase crash risk. Hence, this chapter first identified the key segment (milepost from 12.1 to 13.3 on westbound SR 408), in which a weaving segment exists. Weaving segments have been proven to have higher crash potential than other segment types (see Chapter 4).

Subsequently, a VISSIM network was built based on the geometric characteristics of a study segment and the corresponding MVDS traffic data on Thursdays in August 2015. In order to verify that the traffic condition of the simulation network was consistent with that of the field network, the simulation network was calibrated and validated. The results showed that both the calibration and validation requirements were satisfactorily met.

7 Traffic Safety Improvement for a Congested Weaving Segment

7.1 Introduction

Once the crash mechanisms of weaving segments have been found, countermeasures can be proposed based on crash mechanisms. One possible method to improve the safety of weaving segments is ATM, which is able to dynamically manage roadway facilities based on the prevailing and predicted traffic conditions. Plenty of practitioners and researchers have proven that ATM has the capability to provide safer and smoother traffic (Abdel-Aty et al., 2006; Bhouri & Kauppila, 2011). Among ATM strategies, RM and VSL are widely used approaches. The basic concept of the RM algorithm is adjusting on-ramp entering volume based on the mainline's traffic operational conditions. As for the VSL, the speed limit usually changes according to traffic or weather conditions.

7.2 ATM Strategy Algorithm

7.2.1 Ramp Metering Algorithm

The concept behind the traditional ALINEA is to determine an on-ramp metering rate by the road occupancy observed at the downstream of a merge area and a pre-specified critical occupancy (Papageorgiou et al., 1991). This study adopts a modified ALINEA that additionally considers safety conditions. The RM rate is based on occupancy and the crash risk of the studied weaving segment. Previous studies stated that the occupancy detector should be placed at a location where the congestion caused by on-ramp traffic can be detected, and put the occupancy detector between 130 feet and 1,640 feet downstream of on-ramp noses (Chu & Yang, 2003). This study put the occupancy detector 330 feet downstream of the on-ramp nose.

The metering rate at time step *k* is calculated in Equation (7.1):

$$r(k) = r(k-1) + K_R(\hat{o} - o_{k-1}) + K_s(\hat{p} - p_{k-1}) \tag{7.1}$$

where $r(k)$ is the metering rate (veh/h) at time interval *k*, $r(k-1)$ the metering rate at the previous time interval *k-1*, K_R the occupancy regulator parameter (veh/h), $\hat{o}$ the critical occupancy (%), o_{k-1} the occupancy (%) at time interval *k-1*, K_S the safety regulator parameter (veh/h), p_{k-1} the crash risk at the time interval *k-1*, and $\hat{p}$ the critical crash risk.

The RM is achieved by adjusting the timing of the ramp signal, which is set at the end of the on-ramp. The metering signal permits on-ramp vehicles to enter the weaving segment only when the signal turns green. Otherwise, vehicles are required to stop at the signal and wait for a green phase. The green-phase duration at time interval *k*, $g(k)$, is calculated as follows:

$$g(k) = \left(\frac{r(k)}{r_{sat}}\right).C \tag{7.2}$$

$$g_{\min} \le g(k) \le g_{\max} \tag{7.3}$$

where *C* is the fixed cycle time (10 seconds), r_{sat} the ramp saturation flow (1800 veh/(h.lane)) (Bhouri et al., 2013), g_{min} is 3 seconds, and g_{max} the maximum green-phase duration (10 seconds). Meanwhile, in order to prevent the RM rate from increasing greatly and resulting in a large amount of vehicles entering the mainline at time interval k, the maximum increment of $r(k)$ for each time interval is set to be 60 veh/h.

7.2.2 Variable Speed Limit Strategy

The crash analysis model for weaving segments in Chapter 5 found that the speed difference between the upstream and downstream of a segment is positively related to the crash risk of this segment. Meanwhile, several studies have found that VSL is capable of reducing speed variation (Rämä, 1999; Kwon et al., 2007). Hence, the implementation of VSL might reduce crash risk. In this study, when crash risk is higher than the critical crash risk ($\hat{p}$), VSL at the upstream and the downstream of the congested weaving segment are activated to reduce the speed difference between the beginning and the end of the weaving segment.

7.3 Experiment Design

There were four parameters in the modified ALINEA algorithm that needed to be calibrated: the critical occupancy ($\hat{o}$), the occupancy regulator parameter (K_R), the critical crash risk ($\hat{p}$), and the safety regulator parameter (K_S). These parameters were set as follows:

1. In previous studies, the critical occupancy ($\hat{o}$) was set between 17% and 23%, and it has been found that a higher value of the critical occupancy ensures better safety benefits (Abdel-Aty et al., 2007). For this study, the critical occupancy was set to be 23%.
2. The range of the occupancy regulator parameter (K_R) used in previous studies varied from 70 to 120 veh/h. But it did not have significant effects on the metering rate (Papamichail et al., 2010). This study used 70 veh/h.
3. In order to reduce the false alarm percentage, the threshold ($\hat{p}$) of identifying a crash is set to be 0.15. When the threshold is 0.15, the specificity of the crash estimation model in the previous chapter was 0.973, and the false positive rate was 0.027. That meant only 2.7% of non-crash events were falsely identified as crash events.
4. The safety regulator parameter (K_S) was set to be 0 and then to be 2.5×10^3. Setting the value of K_S is very important. If the value K_S is too small, the crash risk would not have a significant impact on RM rate; if the value is too large, the RM rate might substantially change because of a small variation in crash risk. When K_S was set to be 0, the ALINEA algorithm was the same as the traditional ALINEA algorithm. This study supposes that when the conditional crash risk reaches the highest value, the RM rate is decreased by 180 veh/h, that is one second of green phase time. The maximum conditional crash risk for the weaving segment without ATM control is around 0.22. Then,

$$K_s\left(\hat{p}-p_{\max}\right)=-180 \tag{7.4}$$

$$K_s=\frac{-180}{\hat{p}-p_{\max}}=\frac{-180}{0.15-0.22}\approx 2.5\times 10^3 \tag{7.5}$$

RM might result in long travel times for on-ramp vehicles (Kotsialos & Papageorgiou, 2004). Hence, there was a need to increase the green phase time when there were plenty of vehicles piling up on ramps. The updated green phase time (g') was set as

$$g'=\begin{cases} g & Queue\le 10 \\ g+1 & 10<Queue\le 20 \\ g+2 & 20<Queue\le 30 \\ g+3 & Queue>30 \end{cases} \tag{7.6}$$

where g is calculated based on Equation (7.2), and Queue is the number of vehicles in the queue of the on-ramp. On the other hand, merely increasing the green phase time might not be enough, as entering vehicles needed sufficient gaps in order to merge into the mainline. Hence, it may be better to simultaneously set the upstream variable speed limit in order to provide a bigger gap for entering vehicles.

The parameters used to determine the ramp metering rate were collected from the data collection points in the VISSIM simulation network. Then the COM interface implemented Visual Basic for Applications (VBA) from Excel to adjust the green and red signal timing of RM.

The field speed limit of the studied weaving segment is 55 mph. The speed limit at the upstream was set to be 45, 50, or 55 mph. The speed limit at the downstream was set to be 55, 60, or 65 mph. The application of VSL in microsimulation is carried out by changing the desired speed distributions. The field desired speed data can be obtained from the MVDS detectors on the studied weaving segment. As for other desired speed distributions of VSLs, it is supposed that if the speed limit changes (by decreasing or increasing) by n mph, all vehicles' speeds will accordingly change by n mph. Hence, based on this assumption and the field desired speed distribution, the desired speed distributions of different speed limits can be obtained.

The locations of RM and VSLs are shown in Figure 7.1. The detectors were used to measure the occupancy (o), and data collection points collected other traffic information, i.e., traffic count and speed.

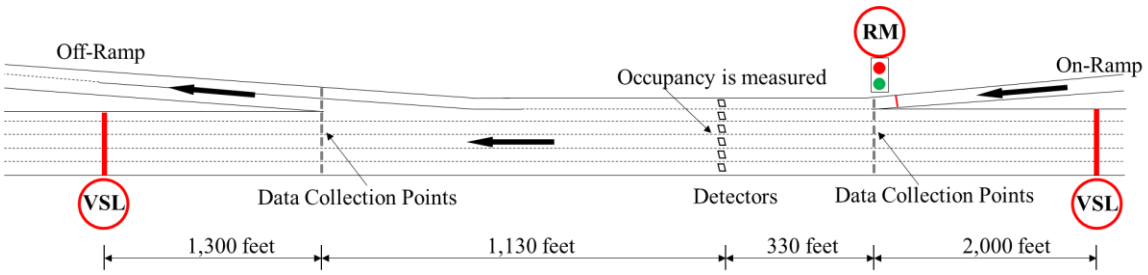

Figure 7.1 – Studied weaving segment microsimulation network.

There were 13 cases in total; the detailed information is listed in Table 7.1. Case 1 is the non-control case, Cases 2-4 are RM strategies, Cases 5-12 are VSL strategies, and Case 3 is the integrated RM-VSL strategy.

Table 7.1 – ATM scenarios.

Case	VSL	RM
1	N/A*	N/A
2	N/A	Ks=0
3	N/A	Ks=2.5×10^6 (without controlling queue)
4	N/A	Ks=2.5×10^6 (Control Queue, Equation 7-6)
5	Upstream 50 mph, Downstream 55 mph	N/A
6	Upstream 45 mph, Downstream 55 mph	N/A
7	Upstream 55 mph, Downstream 60 mph	N/A
8	Upstream 55 mph, Downstream 65 mph	N/A
9	Upstream 50 mph, Downstream 60 mph	N/A
10	Upstream 45 mph, Downstream 60 mph	N/A
11	Upstream 50 mph, Downstream 65 mph	N/A
12	Upstream 45 mph, Downstream 65 mph	N/A
13	Upstream 45 mph, Downstream 55 mph	Ks=2.5×10^6 (Control Queue, Equation 7-6)

*N/A: Not Applicable

7.4 Evaluation of ATM Strategies

All traffic parameters' values can be obtained from VISSIM by data collection points, and the weaving configuration was from the geometric characteristics of the studied weaving segment. The Wet condition of the simulated weaving segment was assumed to be 0. Then, the cumulative odds ratio can be obtained for each simulation run,

$$\overline{OR}_j = \frac{\sum_i (OR)_{ij}}{N} \tag{7.7}$$

where OR_{ij} is the crash odds ratio during the i^{th} time slice in the j^{th} simulation run, N is the number of observations, and each observation was at a five-minute interval.

Ten simulation runs were conducted to eliminate random effects. After excluding 30 minutes of VISSIM warm-up time and 30 minutes of cool-down time, 180 minutes of VISSIM data was put into use. The average cumulative odds ratio over 10 simulation runs for each case was computed. Additionally, in the simulation, the study adopted the Surrogate Safety Assessment Model (SSAM) to provide conflict count, which has proven to be highly correlated with field crash frequency (Shahdah et al., 2014). In each simulation, there existed "virtual" crashes whose time to collision (TTC) was 0. These cases were the result of inaccurate and incomplete logic in the simulation models. Hence, as Gettman et al. (2008) did in their study, these "TTC=0" cases

were excluded from further analysis. Meanwhile, average travel time was obtained to check the network's efficiency. The average results over 10 simulation runs are shown in Table 7.2.

Overall, compared to the non-control case (Case 1), the safety of the congested weaving segment was improved by the ATM strategies. For 9 out of 12 cases, their conflict numbers were reduced and the average odds ratios were less than 1. In addition to improving the safety at the weaving segment, the safety of the non-weaving segments, which were located upstream and downstream of the weaving segment, was also improved significantly (more than 10%) in 7 out of 12 cases. Except for three cases (i.e., 2, 7, and 8), the average travel time of most cases increased because on-ramp vehicles were delayed or the average speed was reduced or both.

Table 7.2 – ATM simulation results

Case	Weaving			Non-weaving		Whole	
	Conflict	Conflict reduced %	$\overline{OR}$	Conflict	Conflict reduced %	ATT#	ATT reduced %
1	705	N/A*	1.00	59	N/A	98.3	N/A
2	653	-7.3	1.01	38	-35.6	97.9	-0.4
3	555	-21.2	0.95	41	-30.5	113.7	15.7
4	621	-11.9	0.92	40	-31.7	101.4	3.2
5	639	-9.3	0.88	62	5.8	100.1	1.9
6	575	-18.4	0.82	43	-26.9	101.3	3.1
7	705	0.1	1.00	59	-0.3	97.7	-0.5
8	705	0.0	1.00	60	1.4	97.4	-0.8
9	639	-9.3	0.88	63	7.7	99.8	1.5
10	575	-18.4	0.82	44	-25.2	101.1	2.9
11	639	-9.3	0.88	63	7.8	99.6	1.4
12	575	-18.4	0.82	43	-26.1	101.0	2.8
13	586	-16.8	0.94	43	-27.6	105.0	6.9

* N/A: Not Applicable

Average Travel Time in seconds

In the traditional ALINEA case (Case 2), the average conflict count was decreased by 7.3%, but the average odds ratio was 1.01, which means the crash odds increased by 1%. On the other hand, the modified ALINEA without controlling queue length (Case 3) decreased conflict by 21.2% and decreased odds by 5%. And for the modified ALINEA whose queue length was controlled (Case 4), it decreased conflict by 11.9% and decreased odds 8%. Since the modified ALINEA cases (i.e., 3 and 4) adjusted the RM rate based on traffic operation and safety conditions simultaneously, they were able to better improve safety than the traditional ALINEA (Case 2). Though the safety benefit of the modified ALINEA without controlling queue length (Case 3) performed well among ALINEAs, the good performance was at the cost of travel time. It increased the average travel time by 15.7%.

Examination of the results in Table 7.2 clearly shows that setting VSL at the downstream of the weaving segment did not improve the safety of the weaving segment. The main reason was that the high speed limit at the downstream of weaving segment does not necessarily increase the speed at the end of the weaving segment, which is mainly impacted by traffic conditions in the

weaving segment. Hence, even though the speed limit at the downstream of the weaving segment was increased, the speed at the end of the weaving segment was still low, the difference between the beginning and the end of the weaving segment remained the same, and the crash risk was almost constant. On the contrary, setting the VSL at the upstream of the weaving segment reduced both conflict number and crash odds. Furthermore, compared to setting the upstream weaving segment VSL to 50 mph, the 45 mph VSL improved the safety more. It is not hard to understand: the lower the speed limit of the upstream segment, the lower the speed at the beginning of the weaving segment, and the lower the speed difference. And the lower speed difference produced lower crash risk.

Though the 45 mph VSL strategy was capable of improving safety without significantly increasing the average travel time, the effectiveness of VSL can be impacted by the compliance level. The VSL system might fail to enhance traffic safety under low compliance conditions (Yu & Abdel-Aty, 2014). In contrast, the modified ALINEA without controlling queue length (Case 3) improved safety at the expense of increased average travel time, but there is no compliance issue for RM. Meanwhile, only controlling the queue length of the modified ALINEA worsened the impact of the modified ALINEA on the weaving segment's safety. Therefore, the RM-VSL was needed to enhance and combine the advantages of VSL and RM. The simulation results demonstrated that the RM-VSL (Case 13) significantly decreased the average travel time by 8.7 seconds when compared to the modified ALINEA without controlling queue length (Case 3). Meanwhile, the RM-VSL (Case 13) was as good as the modified RM without controlling queue length (Case 3) in enhancing the safety of the weaving segment.

Additionally, to test the level of agreement between the conflict count and average odds ratio value, the Spearman's rank correlation test, a non-parametric correlation, was used since there were only 13 cases in total. A higher Spearman's rank correlation coefficient indicates that there is a high dependence between two variables. A coefficient of 1.0 represents a perfect agreement, and that of 0 indicates no correlation (Gettman et al., 2008). The result suggested that the relationship between conflict count and average odds ratio value (Spearman's rank coefficient=0.670, p=0.01) was statistically significant. This confirms that the safety of the simulation is consistent with the crash risk, whose model was built based on field data. But there were still small inconsistencies between conflicts and $\overline{OR}$. The 45 mph VSL (Case 6) was better than the modified ALINEA without controlling queue (Case 3) since Case 6's crash odds compared to the crash odds under base condition were lower than the odds ratio of Case 3. On the other hand, the conflict count of the modified ALINEA without controlling queue (Case 3) was slightly less than that of the 45 mph VSL. Meanwhile, in the modified ALINEA without controlling queue case (Case 3), the percentage of conflict count reduced was higher than the percentage of odds reduced.

Table 7.2 gives cumulative results and does not show detailed information for each step. In order to better understand the effects of ATM strategies on crash risk for each time slice, Figure 7.2 shows the average crash odds ratio of 10 runs for the non-control case (Case 1), the traditional ALINEA (Case 2), the modified ALINEA without controlling queue length (Case 3), 45 mph upstream VSL (Case 6), and RM-VSL (Case 13).

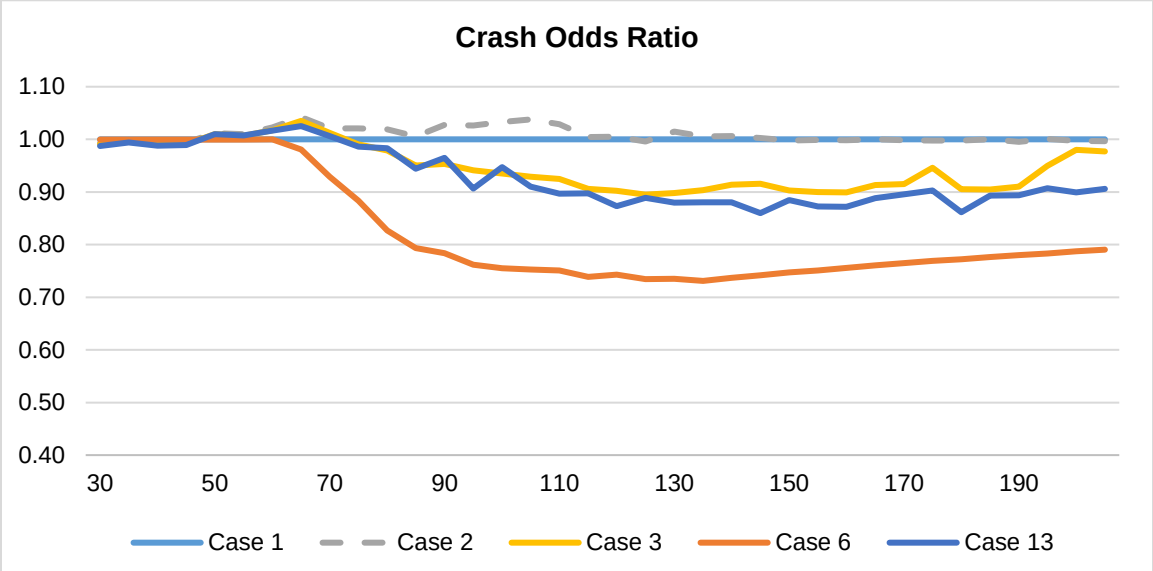

Figure 7.2 – Crash risk for different cases

In Figure 7.2, the crash risk curve of the traditional ALINEA (Case 2) almost overlaps with that of the non-control case (Case 1). This indicates that the traditional ALINEA (Case 2) did not have a significant impact on the safety of the studied weaving segment in each step. The result is not coherent with the previous studies by Lee et al. (2006) and Abdel-Aty and Gayah (2008), which have found that the traditional ALINEA significantly improved real-time safety. This might be because of the difference in study subjects. Their studies focused on freeway segments without distinguishing the segment type, but this study only concentrated on weaving segments. On weaving segments, the traffic behavior and crash mechanisms are not the same as other non-weaving segments.

The crash risk curve of 45 mph VSL (Case 6) is always lower than that of modified RM without controlling queue length (Case 3). It means that the 45 mph VSL outperformed the RM by providing lower crash risks. The reasons might be as follows:

1. When a crash risk is higher than the critical crash risk, the VSL strategy reacts more quickly and effectively than the RM. The speed limit was able to change immediately using VSL; however, the RM adjusted the ramp metering rate gradually.
2. Though RM had the capability to reduce speed variances, the VSL can decrease the variance of speed more. In the simulation run with the random seed of 17, the average speed difference of the non-control case (Case 1) was 6.8 mph, and the average speed differences of the 45 mph VSL (Case 6) and the RM without controlling queue length (Case 3) were 4.6 and 5.7 mph, respectively. Other simulation runs with different random seeds also had similar results.

Another finding from Figure 7.2 is this: when the crash risk was lower than the critical crash risk and the speed limit was returned to 55 mph, the 45 mph VSL at the upstream segment (Case 6) consistently improved the safety of the studied weaving segment. Vehicles did not accelerate significantly and rapidly when the speed limit changed from 45 mph to 55 mph. The vehicles were impacted by vehicles ahead, which were still at low speeds. Meanwhile, when the crash risk was reduced below the critical crash risk, the modified ALINEA without controlling queue length (Case 3) also improved the real-time safety because the metering rate increased gradually and the RM signal broke up platoons of entering vehicles. The same finding also applies to RM-VSL case (Case 13).

7.5 Summary

Traffic conditions in weaving segments are complicated since traffic merges, diverges, and weaves in limited spaces. The complication might result in a low capacity and a high crash risk in weaving segments. In order to improve the safety of a congested weaving segment, ATM strategies were applied in microsimulation. The simulation results show that several ATM strategies were able to improve the safety of the studied weaving segment by providing lower conflict numbers and lower crash odds.

From the perspective of safety, the modified ALINEA cases, which take both traffic operation and safety into consideration, outperformed the traditional ALINEA algorithm. However, the average travel time of the modified ALINEA without controlling queue was significantly higher than the non-control case and also higher than the traditional ALINEA case. The modified ALINEA, which controlled the queue length, shortened the average travel time, but impaired the safety impact of the modified ALINEA algorithm.

Both the location and speed limit value of VSL are important. The VSL set downstream of the studied weaving segment did not mitigate crash risks, but the upstream VSL significantly enhanced the safety of the weaving segment. Meanwhile, the 45 mph VSL improved safety better than the 50 mph VSL without a significant increase in average travel times. Though VSL more effectively improved the safety compared to RMs, the VSLs have the potential problem of compliance, whereas compliance is not a big concern with the RM strategy.

In order to reduce the average travel time of RM and mitigate the compliance issue of VSL, an RM-VSL was proposed. In RM strategy, when the queue of an on-ramp was long, the ramp signal green phase time was increased in order to reduce the queue, and the speed limit upstream of the weaving segment was reduced to 45 mph in order to provide enough time gaps for entering vehicles. The results indicate that the RM-VSL produced lower conflict numbers than the RM with queue control and traditional RM, and that it substantially reduced the average travel time when compared to RM without queue control.

8 Conclusion

The safety of expressways is of significant importance. In order to improve expressway safety, crash-contributing factors were explored in this project. The majority of previous expressway safety studies were based on ADT. If the traffic of an expressway has significant peak and non-peak hours, its crash potential in one segment should be different from another segment, which has the same ADT but the volume is the same for each hour. The studied expressways were mainly used for commuting traffic, which has significant peak and non-peak patterns. Hence, in addition to ADT, this project also applied AHT and microscopic traffic at five-minute intervals to analyze crashes on expressway segments.

In all ADT-based, AHT-based, and microscopic-traffic-based safety studies, the results illustrated that the existence of weaving segment could increase crash potential. It is not hard to understand. Weaving segments are potential recurrent bottlenecks because the capacity of weaving segments is much lower than that of basic expressway segments when controlling for free-flow speed, number of lanes, etc. Meanwhile, they are one of the most complicated segments, since on- and off-ramp traffic merges, diverges, and weaves in limited space. In addition to finding the impact of segment type on safety, the ADT-based, AHT-based, and microscopic-traffic-based safety studies were compared at three levels: total, hourly, and five-minute intervals. The comparison results showed that the microscopic traffic (at five-minute intervals) data was the most suitable traffic data if ATM was used to improve the safety of a segment in real time.

Then, the crash mechanisms of weaving segments were analyzed using real-time safety analysis based on microscopic traffic data at five-minute intervals. The model results showed that the speed difference between the beginning and the end of a weaving segment had significantly positive impacts on the crash risk of the following 5-10 minutes for weaving segments. Meanwhile, the weaving influence length, which was mainly determined by the weaving volume rate, was also positively related to crash potential. These findings indicate that if an ATM strategy is able to reduce speed difference or weaving influence length or both, it could possibly enhance the safety of weaving segments.

A congested weaving segment and its upstream and downstream segments on SR 408 were filtered out to be the key segment of this study. Its average hourly volume in the studied time period in 2015 was 6,521 vehicles, and the average occupancy during peak hours was about 25.0%. The heavy traffic might bring about high crash potential. Hence, this project built a well-calibrated and validated VISSIM network to simulate the traffic condition of the studied weaving segment during peak hours. Two types of ATM strategies, VSL and RM, were applied to the studied weaving segment through COM interface. The simulation result showed that the modified ALINEA cases, which take both traffic operation and safety into consideration, outperformed the traditional ALINEA algorithm in improving safety. Meanwhile, the 45 mph VSL, which was installed upstream of the weaving segment, improved safety better than other VSL strategies.

Though VSL could improve the safety more effectively than RMs, the VSLs have the potential problem of compliance, whereas the compliance is not a big concern in the RM strategy.

Therefore, in order to reduce the average travel time of RM and mitigate the compliance issue of VSL, an RM-VSL was proposed. The results indicate that the RM-VSL produced lower conflict numbers than the RM with queue control and traditional RM, and that it substantially reduced the average travel time compared to RM without queue control.

This project also found that the relationship between the simulated conflict number and the crash odds ratio was statistically significant. However, there were small inconsistencies between the conflict count and the total crash risk. The variance might be due to the difference between crash mechanisms and conflict mechanisms. This finding might inspire further research into the relationship between crash and conflict mechanisms in the real-time perspective.

Overall, this project identified the weaving segments as expressway special facilities that have different crash potential than other segments, found the crash mechanisms of weaving segments, and then applied ATM to improve the safety of a congested weaving segment. In addition to weaving segments, interchanges are also an important expressway facility; they connect expressways with arterials. The traffic in interchanges has different traveling directions and might conflict with each other. Hence, the crash potential in interchanges is high. In recent years, several new types of interchange design have been proposed and built. For example, the diverging diamond interchange (DDI) enables two directions of traffic on the arterials to cross to the opposite side on both sides of the overpass. From the theoretical point of view, the DDI design is able to decrease the number of conflict points and simplify the signal phase. However, it may cause drivers confusion in the initial stages. Thus, the traffic safety of such new interchange design must be thoroughly examined. Furthermore, simulation can also be implemented to suggest better designs to improve the current interchange configuration.

APPENDIX A: MVDS System and Lane Configuration

Table A.1 – SR 408 westbound MVDS system and lane configuration.

Westbound		Number of lanes			Westbound		Number of lanes		
ID	Milepost	Mainline (w/ TP Express)	TP Cash	Ramp	ID	Milepost	Mainline (w/ TP Express)	TP Cash	Ramp
1	1.2			2	29	11.6	4		1
2	1.4	2			30	12.1	5		
3	1.6	3		2	31	12.6	5		2
4	2	3		1	32	13	5		1
5	2.4	3		1	33	13.3	3	2	
6	2.7	2	1		34	13.6	3	4	1
7	3.2	2	2		35	14.2	5		1
8	3.6	2		1	36	14.4	4		1
9	4.3	3		2	37	14.5	5		
10	4.6	4			38	15.2	5		
11	4.9	3		1	39	15.7	5		1
12	5.3	3		1	40	15.9	4		1
13	5.9	3	2	1	41	16.1	4		2
14	6.3	3	2		42	16.5	5		
15	6.8	3			43	17	3		2
16	7.3	3		1	44	17.8	3		1
17	7.4	4			45	18	3		1
18	7.6	3		1	46	18.4	2		1
19	8.1	3		1	47	18.8	2		1
20	8.4	3		1	48	19	2	1	
21	8.9	3		1	49	19.4	2	2	
22	9.2	3		1	50	19.7	3		1
23	9.7	3		1	51	19.9	2		1
24	9.9	2		2	52	20.7	3		
25	10.3	3		1	53	20.8	2		1
26	10.6	4			54	21.8	2		
27	10.9	4		2	55	22.3	2		1
28	11.3	5		1	56	22.7	2		1

Table A.2 – SR 417 northbound MVDS system and lane configuration.

Northbound		Number of lanes			Northbound		Number of lanes		
ID	Milepost	Mainline (w/ TP Express)	TP Cash	Ramp	ID	Milepost	Mainline (w/ TP Express)	TP Cash	Ramp
1	5.9	2			29	23.9	2		1
2	6.2	2		2	30	24.5	2		
3	7.2	2	2		31	25	2		1
4	7.5	2	1		32	26.1	2		3
5	8.2	2			33	26.9	4		
6	9.4	2		1	34	27.3	3		2
7	10.1	2		1	35	27.9	3		1
8	10.6	2		1	36	28.1	3	2	
9	11	2		2	37	28.5	3	1	
10	12.2	2			38	28.7	4		
11	13.1	3		2	39	29.5	3		1
12	13.9	2		1	40	30.2	2		1
13	14.5	2			41	31.2	2		
14	15.2	4			42	31.9	2		
15	15.6	2	1		43	32.5	2		1
16	16.4	2			44	33			1
17	16.6	2		1	45	33.3	4		1
18	17.9	2		1	46	33.6	4		
19	18.2	2			47	34	3		2
20	18.8	2		1	48	34.6	3		1
21	19.3	2		1	49	35.2	3		
22	20.4	2			50	35.5	2	2	
23	20.9	2			51	36	3	2	
24	21.3	2		1	52	36.4	4		2
25	22	2		1	53	36.7	3		1
26	22.5	2		1	54	36.9	3		1
27	23	2		1	55	37.2	3		
28	23.6	2		1	56	37.7	2		

Table A.3 – SR 417 southbound MVDS system and lane configuration.

Southbound		Number of lanes			Southbound		Number of lanes		
ID	Milepost	Mainline (w/ TP Express)	TP Cash	Ramp	ID	Milepost	Mainline (w/ TP Express)	TP Cash	Ramp
1	5.9	2			29	24.2	2		1
2	6.2	2		2	30	24.5	2		1
3	7.2	2	1		31	24.9	2		1
4	7.5	2	2		32	26.1	3		2
5	8.2	2			33	26.9	4		
6	9.4	2		1	34	27.3	3		1
7	10.3	2		2	35	27.9	4		1
8	10.7	2		1	36	28.1	3	1	
9	11.2	3		1	37	28.5	3	2	
10	12.2	2			38	28.7	4		
11	13.2	2		1	39	29.5	3		1
12	13.9	2		1	40	30.2	2		1
13	14.7	2			41	31.2	2		
14	15.2	3			42	31.9	2		
15	15.6	2	2		43	32.5	2		1
16	16.4	2			44	32.9			1
17	16.6	2		1	45	33.1	3		2
18	17.7	2		1	46	33.6	3		2
19	18.2	2			47	34.5	3		1
20	18.8	2		1	48	34.8	3		1
21	19.5	2		1	49	35.2	3		
22	20.4	2			50	35.5	2	1	
23	20.9	2			51	36	2	2	
24	21.3	2		1	52	36.4	3		1
25	22.2	2		1	53	36.7	2		1
26	23	3			54	37	2		1
27	23.2	2		1	55	37.2	2		
28	23.5	2		1	56	37.7	2		

Table A.4 – SR 528 eastbound MVDS system and lane configuration.

Eastbound		Number of lanes			Eastbound		Number of lanes		
ID	Milepost	Mainline (w/ TP Express)	TP Cash	Ramp	ID	Milepost	Mainline (w/ TP Express)	TP Cash	Ramp
1	8.5	3		1	16	15.3			3
2	9	3		1	17	15.7			2
3	9.5	3		1	18	15.9	2		2
4	9.8	3			19	16.6	2	2	
5	10.3	2		3	20	17.2	2	2	
6	10.7	2		1	21	19.5	2		1
7	10.8			1	22	20.2	2		1
8	11.1	2		1	23	23.2	2		
9	11.7	3		1	24	23.5	2		1
10	12.5	3		1	25	25.9	2	2	
11	12.8	4			26	26.3	2	1	
12	13.2	3		2	27	28.6	2		
13	13.8	2		1	28	30.6	2		1
14	14.5	2			29	31.9	2		
15	15	2		2					

Table A.5 – SR 528 westbound MVDS system and lane configuration.

Westbound		Number of lanes			Westbound		Number of lanes		
ID	Milepost	Mainline (w/ TP Express)	TP Cash	Ramp	ID	Milepost	Mainline (w/ TP Express)	TP Cash	Ramp
1	8.5	3		1	16	15.3	2		2
2	9.4	3		1	17	15.6	2		1
3	9.5	3		1	18	15.9	2		2
4	9.8	3			19	16.6	2	2	
5	10.3	4			20	17.2	2	2	
6	10.5	2		2	21	19.5	2		1
7	10.9	2		1	22	20.2	2		1
8	11	3		2	23	23.3	2		
9	12	4		1	24	23.5	2		1
10	12.2	3		1	25	25.9	2	1	
11	12.5	3		1	26	26.3	2	2	
12	12.8	3			27	28.6	2		
13	13.2	3		1	28	30.6	2		1
14	13.8	3		1	29	31.9	2		
15	14.5	2							

APPENDIX B Expressway Hourly Volume

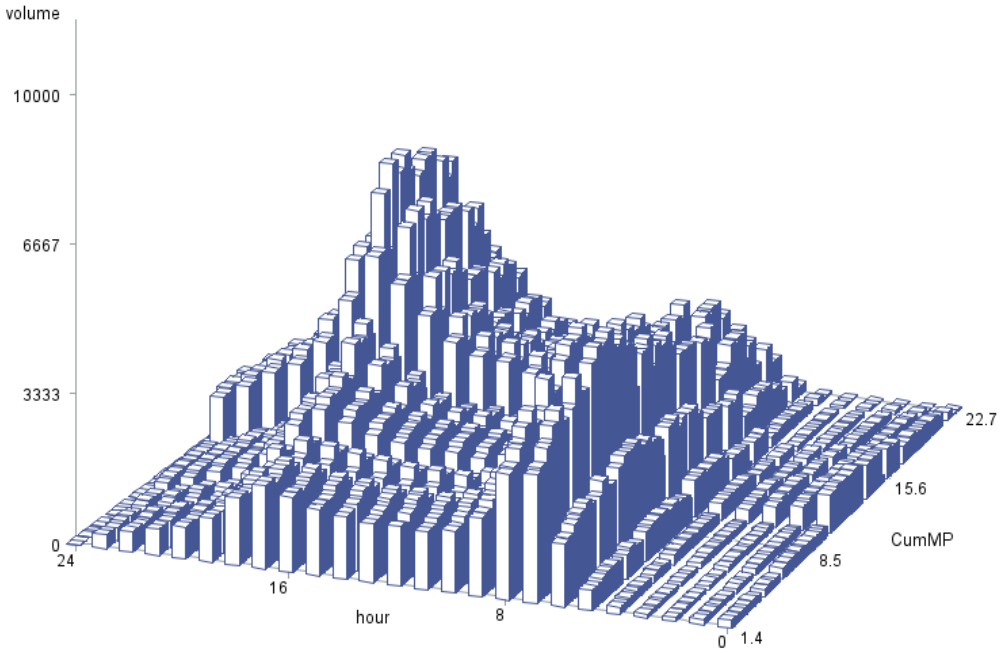

Figure B.1 – Weekday hourly volume of SR 408 eastbound in August 2015.

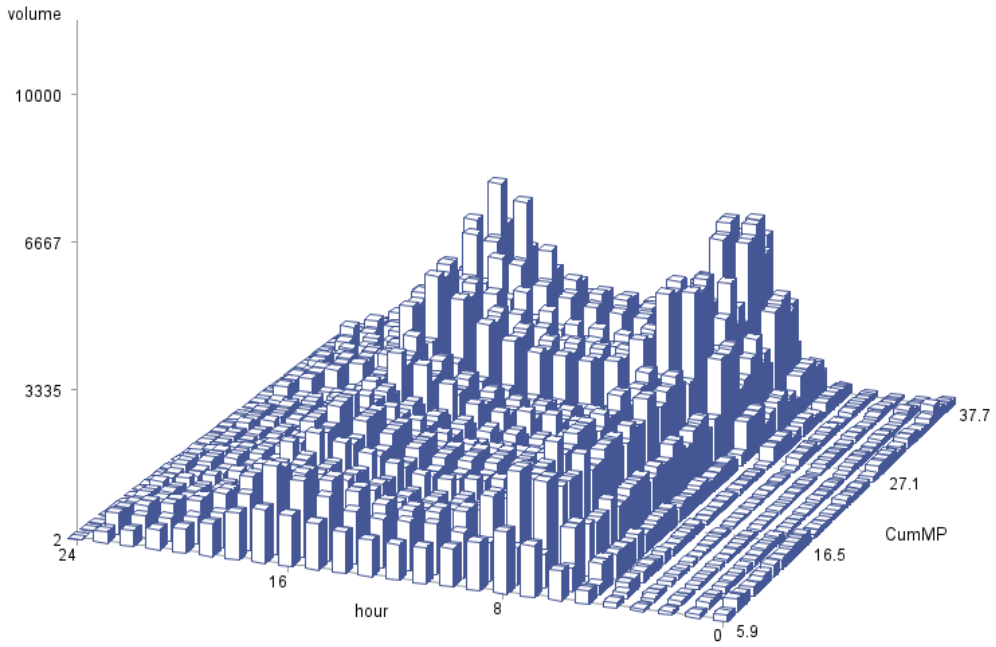

Figure B.2 – Weekday hourly volume of SR 417 southbound in August 2015.

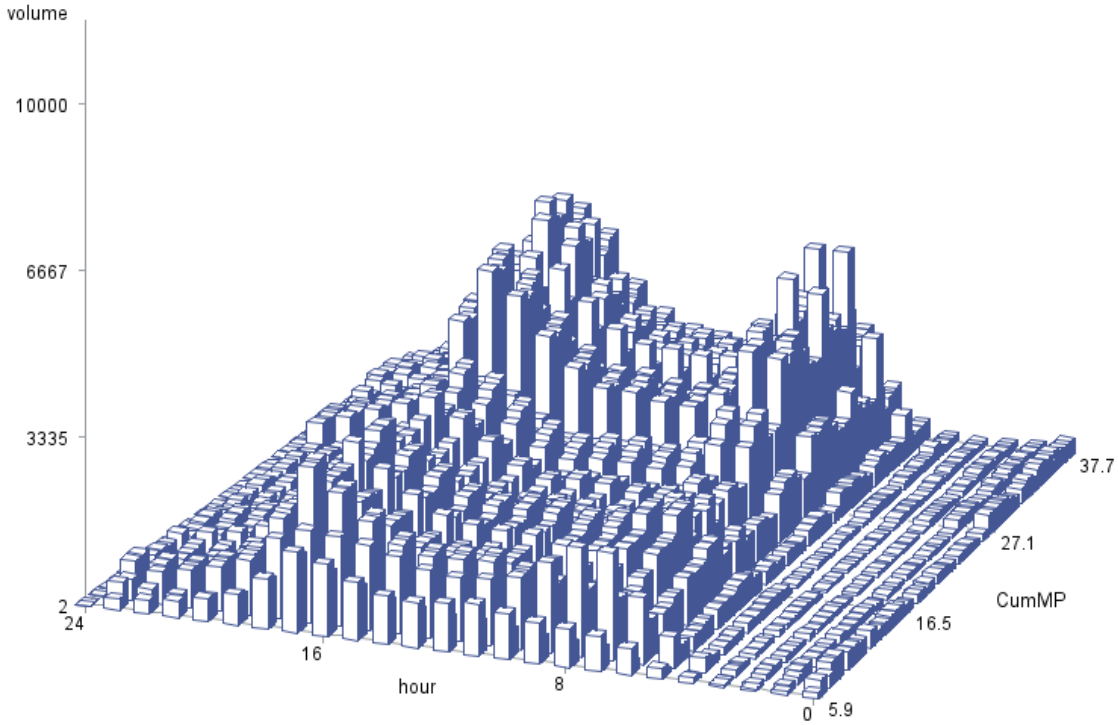

Figure B.3 – Weekday hourly volume of SR 417 northbound in August 2015.

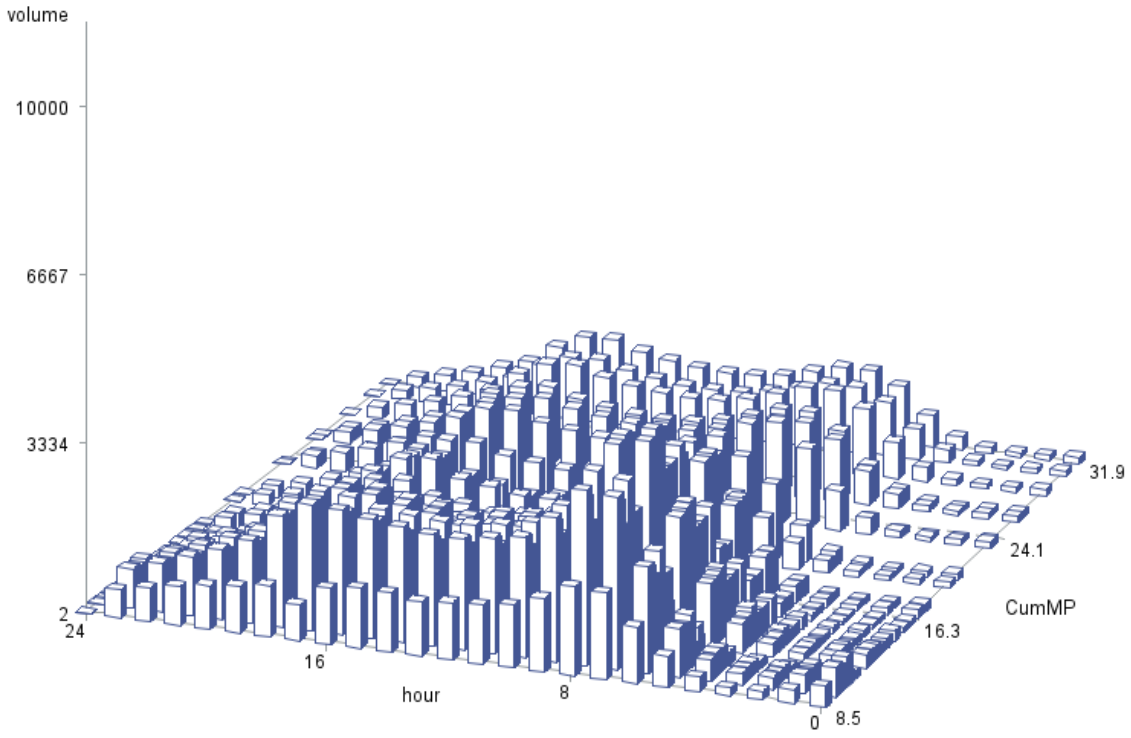

Figure B.4 – Weekday hourly volume of SR 528 westbound in August 2015.

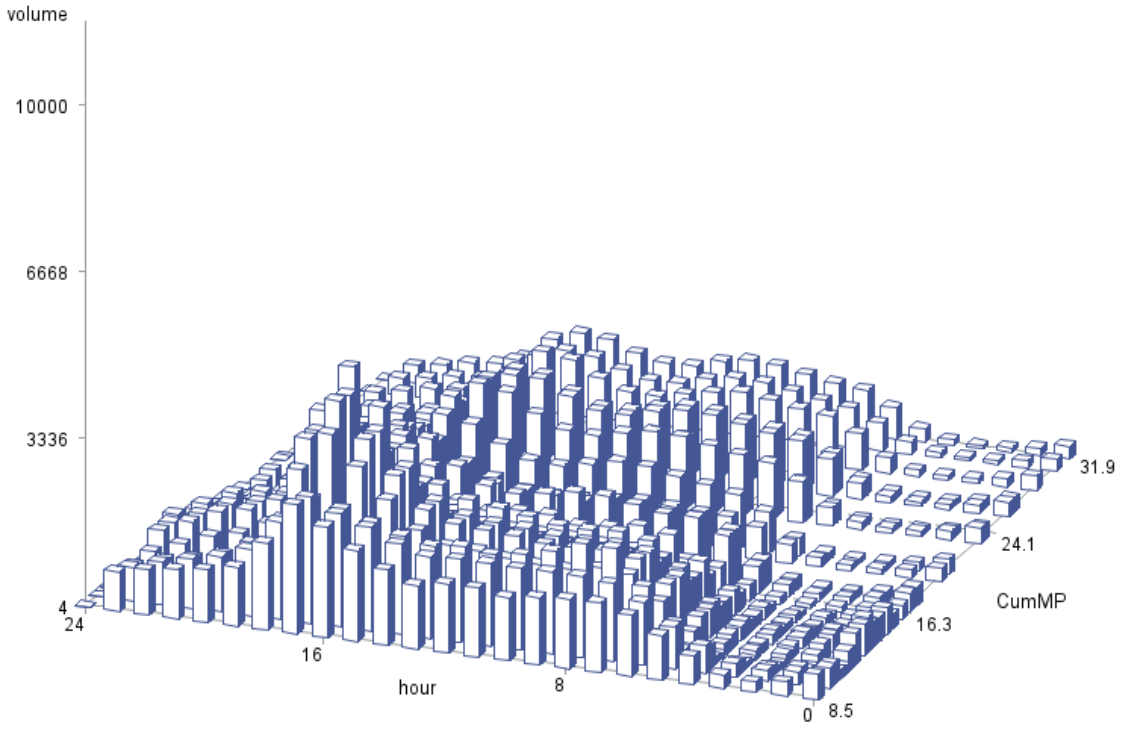

Figure B.5 – Weekday hourly volume of SR 528 eastbound in August 2015 .

APPENDIX C: Expressway Mainline Congestion

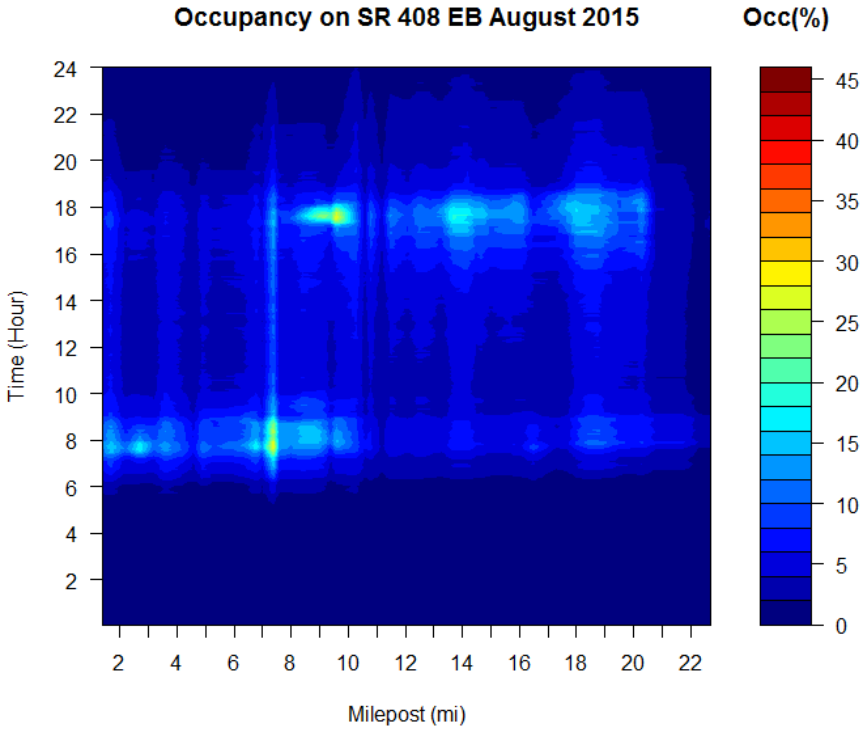

Figure C.1 – Weekday occupancy of SR 408 eastbound.

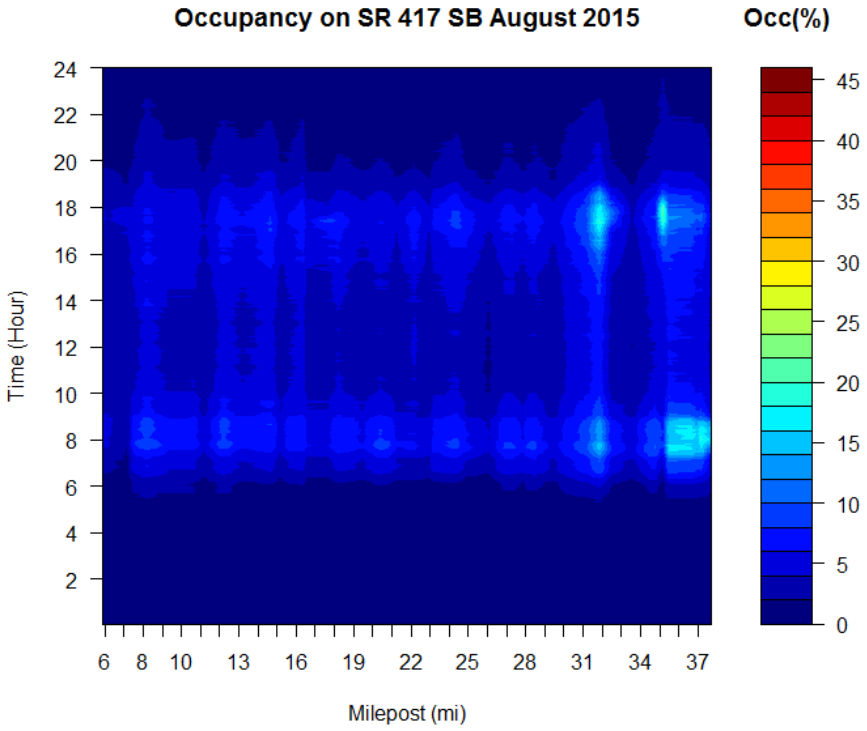

Figure C.2 – Weekday occupancy of SR 417 southbound.

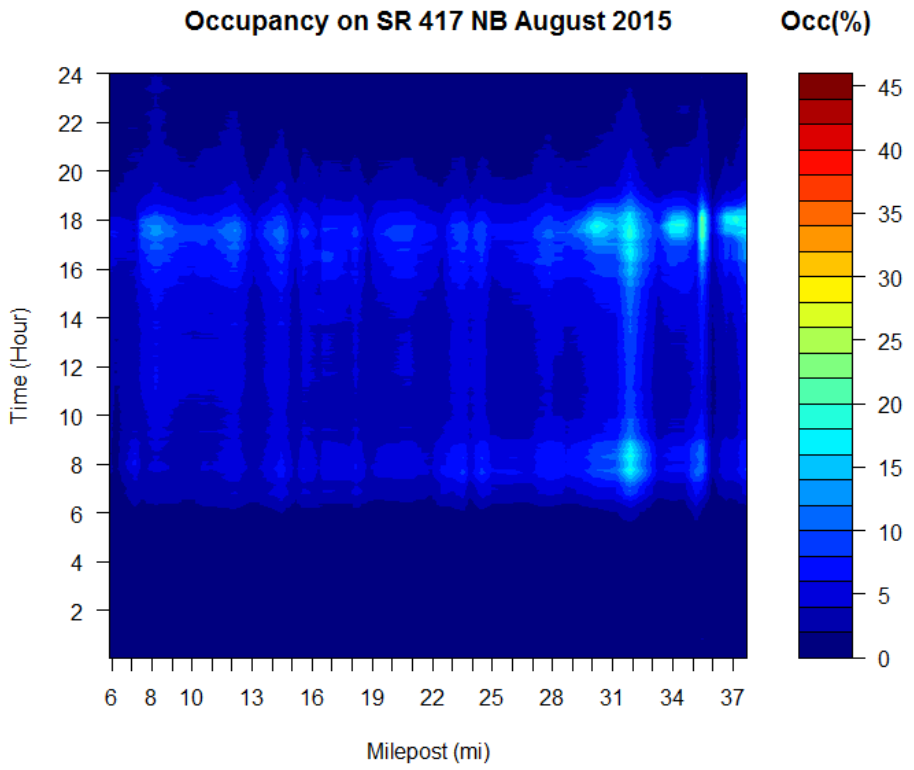

Figure C.3 – Weekday occupancy of SR 417 northbound.

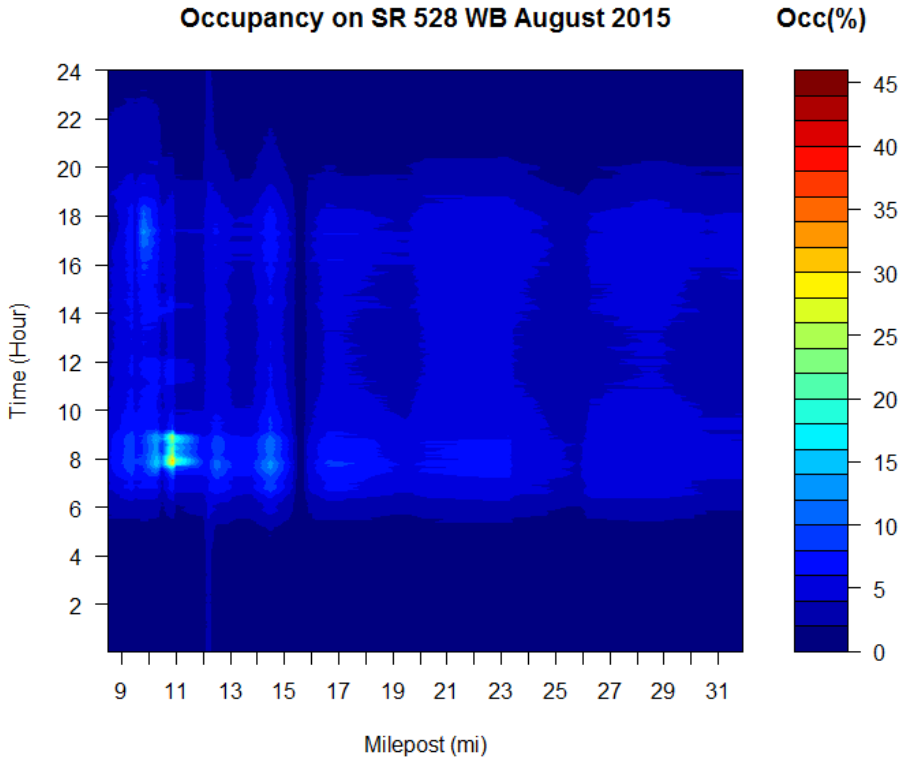

Figure C.4 – Weekday occupancy of SR 528 westbound.

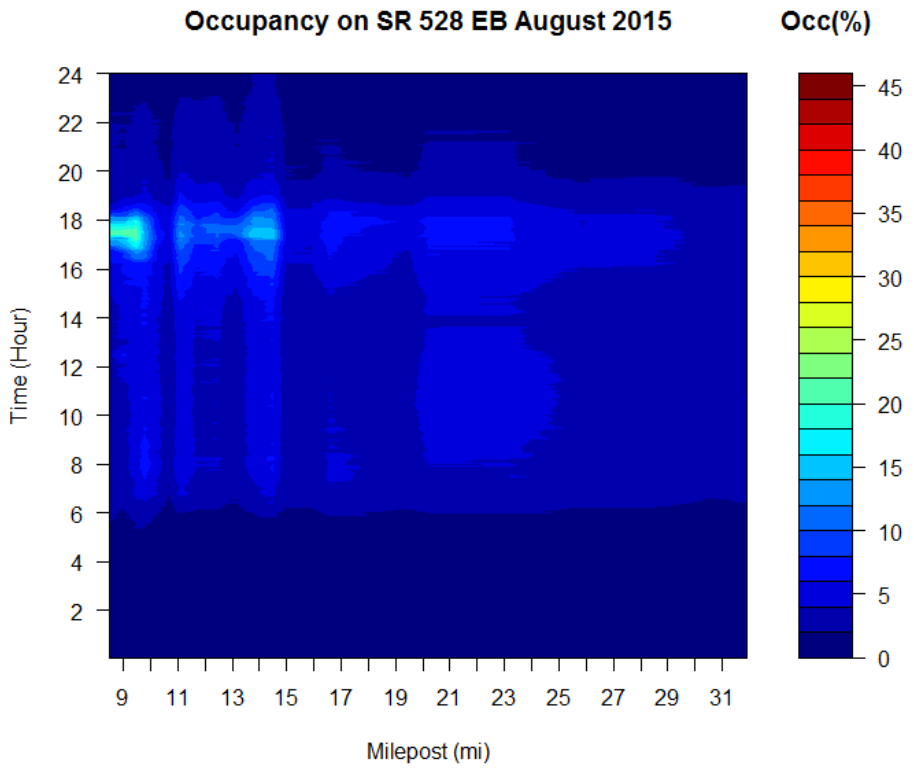

Figure C.5 – Weekday occupancy of SR 528 eastbound.

9 References

Abdel-Aty, M., Dhindsa, A., & Gayah, V. (2007). Considering various alinea ramp metering strategies for crash risk mitigation on freeways under congested regime. *Transportation Research Part C: Emerging Technologies,* 15 (2), 113-134.

Abdel-Aty, M., & Dhindsa, A. (2007). Coordinated use of variable speed limits and ramp metering for improving safety on congested freeways. In: *Proceedings of the Transportation Research Board 86th Annual Meeting*, Washington, DC.

Abdel-Aty, M., Dilmore, J., & Dhindsa, A. (2006). Evaluation of variable speed limits for real-time freeway safety improvement. *Accident Analysis & Prevention,* 38 (2), 335-345.

Abdel-Aty, M., & Gayah, V. (2008). Comparison of two different ramp metering algorithms for real-time crash risk reduction. In: *Proceedings of the Transportation Research Board 87th Annual Meeting*, Washington, DC.

Abdel-Aty, M., Haleem, K., Cunningham, R., & Gayah, V. (2009). Application of variable speed limits and ramp metering to improve safety and efficiency of freeways. In: *Proceedings of the 2nd International Symposium on Freeway and Tollway Operations*, Honolulu, Hawaii.

Abdel-Aty, M., & Pemmanaboina, R. (2006). Calibrating a real-time traffic crash-prediction model using archived weather and its traffic data. *IEEE Transactions on Intelligent Transportation Systems,* 7 (2), 167-174.

Abdel-Aty, M., Uddin, N., & Pande, A. (2005). Split models for predicting multivehicle crashes during high-speed and low-speed operating conditions on freeways. *Transportation Research Record: Journal of the Transportation Research Board* (1908), 51-58.

Abdel-Aty, M., Uddin, N., Pande, A., Abdalla, F., & Hsia, L. (2004). Predicting freeway crashes from loop detector data by matched case-control logistic regression. *Transportation Research Record: Journal of the Transportation Research Board* (1897), 88-95.

Bhouri, N., Haj-Salem, H., & Kauppila, J. (2013). Isolated versus coordinated ramp metering: Field evaluation results of travel time reliability and traffic impact. *Transportation Research Part C: Emerging Technologies* 28, 155-167.

Bhouri, N., & Kauppila, J. (2011). Managing highways for better reliability: Assessing reliability benefits of ramp metering. *Transportation Research Record: Journal of the Transportation Research Board* (2229), 1-7.

Cambridge Systematics Inc. (2001). *Final report: Twin cities ramp meter evaluation*. Retrieved September 13, 2016, from http://ntl.bts.gov/lib/jpodocs/repts_te/13425.pdf.

Cassidy, M.J., & Rudjanakanoknad, J. (2005). Increasing the capacity of an isolated merge by metering its on-ramp. *Transportation Research Part B: Methodological*, 39 (10), 896-913.

Ceder, A. (1982). Relationships between road accidents and hourly traffic flow—ii: Probabilistic approach. *Accident Analysis & Prevention*, 14 (1), 35-44.

Central Florida Expressway Authority (CFX). (2016). Maps. Retrieved September 9, 2016, from https://www.cfxway.com/TravelersExpressways/TravelResources/Maps.aspx.

Chang, J., Oh, C., & Chang, M. (2000). Effects of traffic condition (v/c) on safety at freeway facility sections. In: *Proceedings of the Transportation Research, E-Circular: 4th International Symposium on Highway Capacity,* Maui, Hawaii.

Chu, L., & Yang, X. (2003). Optimization of the ALINEA ramp-metering control using genetic algorithm with micro-simulation. In: *Proceedings of the Transportation Research Board 82nd Annual Meeting*, Washington, DC.

Dowling, R., Skabardonis, A., & Alexiadis, V. (2004). Traffic analysis toolbox volume III: Guidelines for applying traffic microsimulation modeling software. Report: FHWA-HRT-04-040

Federal Highway Administration (FHWA). (2014). How Do Weather Events Impact Roads? Retrieved September 9, 2016, from http://ops.fhwa.dot.gov/Weather/q1_roadimpact.htm.

Gelman, A., Carlin, J.B., Stern, H.S., & Rubin, D.B. (2014). *Bayesian data analysis*. CRC Press.

Gelman, A., & Hill, J. (2006). *Data Analysis Using Regression and Multilevel/Hierarchical Models*. Cambridge: Cambridge University Press.

Gettman, D., Pu, L., Sayed, T., & Shelby, S.G. (2008). *Surrogate safety assessment model and validation: Final report*. Report: FHWA-HRT-08-051.

Gwynn, D.W. (1967). Relationship of accident rates and accident involvements with hourly volumes. *Traffic Quarterly*, 21 (3), 407-418.

Haj-Salem, H., & Papageorgiou, M. (1995). Ramp metering impact on urban corridor traffic: Field results. *Transportation Research Part A: Policy and Practice*, 29 (4), 303-319.

Hall, F.L. (1996). Traffic stream characteristics. In *Traffic Flow Theory* (monograph). Washington, DC: US Federal Highway Administration.

Hegyi, A., De Schutter, B., & Hellendoorn, H. (2005). Model predictive control for optimal coordination of ramp metering and variable speed limits. *Transportation Research Part C: Emerging Technologies*, 13 (3), 185-209.

Hosmer D.W., Lemeshow, S., & Sturdivant, R.X. (2013). *Applied logistic regression*. Hoboken, NJ: John Wiley & Sons.

Hossain, M., & Muromachi, Y. (2010). Evaluating location of placement and spacing of detectors for real-time crash prediction on urban expressways. In: *Proceedings of the Transportation Research Board 89th Annual Meeting*, Washington, DC.

Hossain, M., & Muromachi, Y. (2013a). A real-time crash prediction model for the ramp vicinities of urban expressways. *IATSS Research*, 37 (1), 68-79.

Hossain, M., & Muromachi, Y. (2013b). Understanding crash mechanism on urban expressways using high-resolution traffic data. *Accident Analysis & Prevention*, 57, 17-29.

Hourdos, J., Garg, V., Michalopoulos, P., & Davis, G. (2006). Real-time detection of crash-prone conditions at freeway high-crash locations. *Transportation Research Record: Journal of the Transportation Research Board* (1968), 83-91.

Johnson, S., & Murray, D. (2010). Empirical analysis of truck and automobile speeds on rural interstates: Impact of posted speed limits. In: *Proceedings of the Transportation Research Board 89th Annual Meeting*, Washington, DC.

Kang, K.-P., & Chang, G.-L. (2011). An integrated control algorithm of the advanced merge and speed limit strategies at highway work zones. In: *Proceedings of the Transportation Research Board 90th Annual Meeting*, Washington, DC.

Koppula, N. (2002). A comparative analysis of weaving areas in hcm, transims, corsim, vissim and integration. Thesis, Virginia Polytechnic Institute.

Kotsialos, A., & Papageorgiou, M. (2004). Efficiency and equity properties of freeway network-wide ramp metering with amoc. *Transportation Research Part C: Emerging Technologies,* 12 (6), 401-420.

Kwon, E., Brannan, D., Shouman, K., Isackson, C., & Arseneau, B. (2007). Development and field evaluation of variable advisory speed limit system for work zones. *Transportation Research Record: Journal of the Transportation Research Board* (2015), 12-18.

Lee, C., & Abdel-Aty, M. (2006). Temporal variations in traffic flow and ramp-related crash risk. In: *Proceedings of the 9th Applications of Advanced Technology in Transportation*, Chicago Illinois.

Lee, C., & Abdel-Aty, M. (2008). Testing effects of warning messages and variable speed limits on driver behavior using driving simulator. *Transportation Research Record: Journal of the Transportation Research Board* (2069), 55-64.

Lee, C., Hellinga, B., & Ozbay, K. (2006). Quantifying effects of ramp metering on freeway safety. *Accident Analysis & Prevention,* 38 (2), 279-288.

Lee, C., Hellinga, B., & Saccomanno, F. (2004). Assessing safety benefits of variable speed limits. *Transportation Research Record: Journal of the Transportation Research Board* (1897), 183-190.

Lee, C., Saccomanno, F., & Hellinga, B. (2002). Analysis of crash precursors on instrumented freeways. *Transportation Research Record: Journal of the Transportation Research Board* (1784), 1-8.

Li, D., Ranjitkar, P., & Ceder, A. (2014). A logic tree based algorithm for variable speed limit controllers to manage recurrently congested bottlenecks. In: *Proceedings of the Transportation Research Board 93rd Annual Meeting*, Washington, DC.

Liu, P., Chen, H., Lu, J.J., & Cao, B. (2009). How lane arrangements on freeway mainlines and ramps affect safety of freeways with closely spaced entrance and exit ramps. *Journal of Transportation Engineering*, 136 (7), 614-622.

Lord, D., Manar, A., & Vizioli, A. (2005). Modeling crash-flow-density and crash-flow-v/c ratio relationships for rural and urban freeway segments. *Accident Analysis & Prevention*, 37 (1), 185-199.

Lord, D., & Mannering, F. (2010). The statistical analysis of crash-frequency data: A review and assessment of methodological alternatives. *Transportation Research Part A: Policy and Practice,* 44 (5), 291-305.

Lu, X.-Y., Varaiya, P., Horowitz, R., Su, D., & Shladover, S. (2011). Novel freeway traffic control with variable speed limit and coordinated ramp metering. *Transportation Research Record: Journal of the Transportation Research Board* (2229), 55-65.

Madanat, S., & Liu, P.-C. (1995). *A prototype system for real-time incident likelihood prediction.* ITS-IDEA Program Project Final Report.

Martin, J.-L. (2002). Relationship between crash rate and hourly traffic flow on interurban motorways. *Accident Analysis & Prevention*, 34 (5), 619-629.

Mensah, A., & Hauer, E. (1998). Two problems of averaging arising in the estimation of the relationship between accidents and traffic flow. *Transportation Research Record: Journal of the Transportation Research Board* (1635), 37-43.

Michalopoulos, P., Xin, W., & Hourdos, J. (2005). *Evaluation and improvement of the stratified ramp metering algorithm through microscopic simulation-Phase II.* report: Mn/DOT 2005-48.

National Research Council. (2000). *Highway Capacity Manual.* Washington, DC: Transportation Research Board.

National Research Council. (2010). *HCM 2010: Highway Capacity Manual.* Washington, DC: Transportation Research Board.

Nezamuddin, N., Jiang, N., Zhang, T., Waller, S.T., & Sun, D. (2011). *Traffic operations and safety benefits of active traffic strategies on TXDOT freeways*. Report: FHWA/TX-12/0-6576-1.

Olson, D.L., & Delen, D. (2008). *Advanced data mining techniques*. Berlin: Springer.

Pahukula, J., Hernandez, S., & Unnikrishnan, A. (2015). A time of day analysis of crashes involving large trucks in urban areas. *Accident Analysis & Prevention,* 75, 155-163.

Pande, A., Abdel-Aty, M., & Hsia, L. (2005). Spatiotemporal variation of risk preceding crashes on freeways. *Transportation Research Record: Journal of the Transportation Research Board* (1908), 26-36.

Pande, A., Das, A., Abdel-Aty, M., & Hassan, H. (2011). Estimation of real-time crash risk: Are all freeways created equal? *Transportation Research Record: Journal of the Transportation Research Board* (2237), 60-66.

Papageorgiou, M., Hadj-Salem, H., & Blosseville, J.-M. (1991). ALINEA: A local feedback control law for on-ramp metering. *Transportation Research Record: Journal of the Transportation Research Board* (1320), 58-64.

Papageorgiou, M., & Kotsialos, A. (2000). Freeway ramp metering: An overview. In: *Proceedings of the Intelligent Transportation Systems*, Dearborn, MI.

Papamichail, I., Papageorgiou, M., Vong, V., & Gaffney, J. (2010). Heuristic ramp-metering coordination strategy implemented at Monash Freeway, Australia. *Transportation Research Record: Journal of the Transportation Research Board* (2178), 10-20.

Park, B.-J., Fitzpatrick, K., & Lord, D. (2010). Evaluating the effects of freeway design elements on safety. *Transportation Research Record: Journal of the Transportation Research Board* (2195), 58-69.

Park, J., Abdel-Aty, M., & Lee, J. (2016). Use of empirical and full bayes before–after approaches to estimate the safety effects of roadside barriers with different crash conditions. *Journal of Safety Research,* 58, 31-40.

Persaud, B., & Dzbik, L. (1993). Accident prediction models for freeways. *Transportation Research Record: Journal of the Transportation Research Board* (1401), 55-60.

PTV Group. (2013). *PTV Vissim 6 user manual*. Karlsruhe, Germany: PTV AG.

Pulugurtha, S.S., & Bhatt, J. (2010). Evaluating the role of weaving section characteristics and traffic on crashes in weaving areas. *Traffic Injury Prevention*, 11 (1), 104-113.

Qu, X., Wang, W., Wang, W., Liu, P., & Noyce, D.A. (2012). Real-time prediction of freeway rear-end crash potential by support vector machine. In: *Proceedings of the Transportation Research Board 91st Annual Meeting*, Washington, D.C.

Rämä, P. (1999). Effects of weather-controlled variable speed limits and warning signs on driver behavior. *Transportation Research Record: Journal of the Transportation Research Board* (1689), 53-59.

Ray, B.L., Schoen, J., Jenior, P., Knudsen, J., Porter, R.J., Leisch, J.P., Mason, J., & Roess, R. (2011). *Guidelines for ramp and interchange spacing*. Report: NCHRP 687.

Saha, P., & Young, R.K. (2014). Weather-based safety analysis for the effectiveness of rural vsl corridors. In: *Proceedings of the Transportation Research Board 93rd Annual Meeting*, Washington, D.C.

Shahdah, U., Saccomanno, F., & Persaud, B. (2014). Integrated traffic conflict model for estimating crash modification factors. *Accident Analysis & Prevention* 71, 228-235.

Vittinghoff, E., Glidden, D.V., Shiboski, S.C., & Mcculloch, C.E. (2011). *Regression methods in biostatistics: Linear, logistic, survival, and repeated measures models*. Boston: Springer.

Wang, L., Abdel-Aty, M., Shi, Q., & Park, J. (2015a). Real-time crash prediction for expressway weaving segments. *Transportation Research Part C: Emerging Technologies,* 61, 1-10.

Wang, L., Shi, Q., & Abdel-Aty, M. (2015b). Predicting crashes on expressway ramps with real-time traffic and weather data. *Transportation Research Record: Journal of the Transportation Research Board* (2514), 32-38.

Woody, T. (2006). *Calibrating freeway simulation models in Vissim*. Thesis, University of Washington.

Yu, R., & Abdel-Aty, M. (2013). Multi-level Bayesian analyses for single-and multi-vehicle freeway crashes. *Accident Analysis & Prevention*, 58, 97-105.

Yu, R., & Abdel-Aty, M. (2014). An optimal variable speed limits system to ameliorate traffic safety risk. *Transportation Research Part C: Emerging Technologies*, 46, 235-246.

Zheng, Z., Ahn, S., & Monsere, C.M. (2010). Impact of traffic oscillations on freeway crash occurrences. *Accident Analysis & Prevention*, 42 (2), 626-636.

Zhou, M., & Sisiopiku, V. (1997). Relationship between volume-to-capacity ratios and accident rates. *Transportation Research Record: Journal of the Transportation Research Board* (1581), 47-52.